8TH RILEM INTERNATIONAL CONFERENCE ON MECHANISMS OF CRACKING AND DEBONDING IN PAVEMENTS

June 7 - 9, 2016 – Nantes, FRANCE

Workshop 4 , June 9

Recent progress in Digital Image Correlation: towards integrated identification?

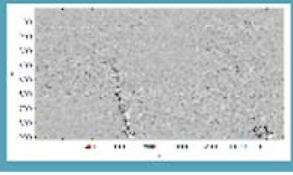

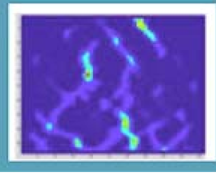

Two civil and industrial applications of 2D DIC measurements combined with numerical simulations

Roberto Fedele and coworkers:
M. Scaioni, G. Rosati. M. Ferraris, V. Casalegno

Department of Civil and Environmental Engineering (DICA)
Politecnico di Milano, Milan, Italy

Items to be discussed

- Delamination tests on FRP-reinforced masonry pillar, optical monitoring by 2D DIC and FE predictions

  coworkers: M. Scaioni, G. Rosati

- Shear tests on metal-ceramic assemblies, identification of cohesive parameters for innovative joints

  coworkers: M. Ferraris, V. Casalegno

- Closing remarks and future prospects

Delamination experiments and FE modelling of FRP-reinforced masonry

Roberto Fedele, M. Scaioni, G. Rosati

Ref: Fedele et alii, Cement & Concrete Composites, 45 (2014) 243–254.

Department of Civil and Environmental Engineering (DICA)
Politecnico di Milano, Milan, Italy

CFRP-reinforced pillar: Historical bricks (XVII century) and high strength mortar

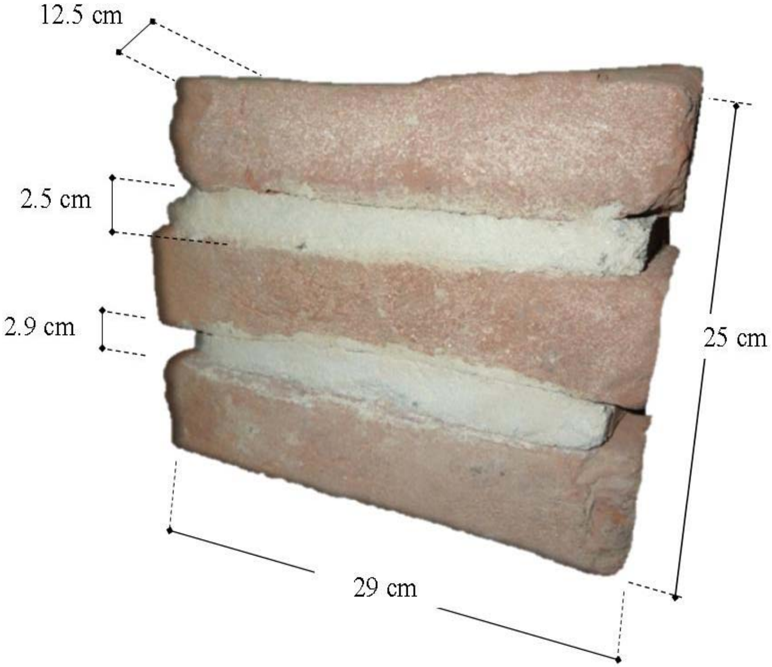

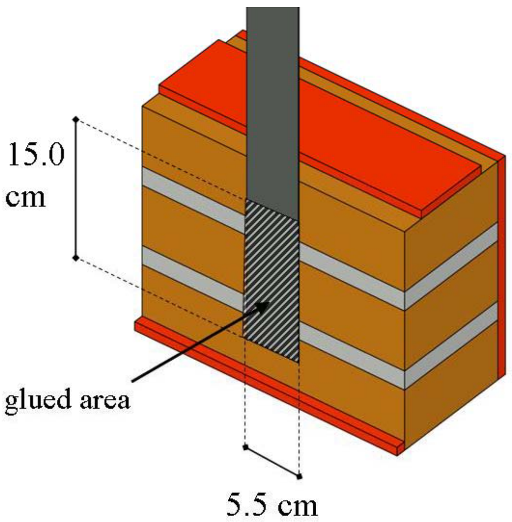

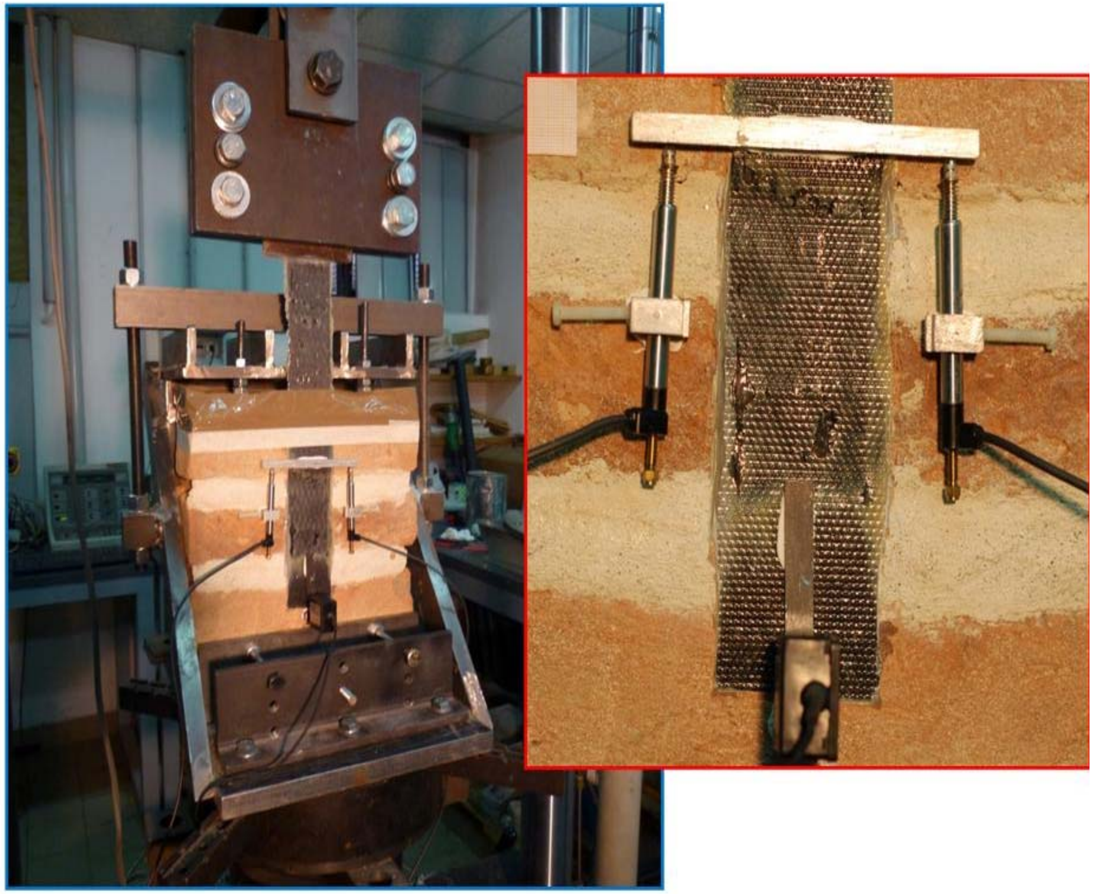

single-lap shear test

Optical monitoring by 2D DIC

1 pixel footprint on the object ≅ 84 μm

metric object space

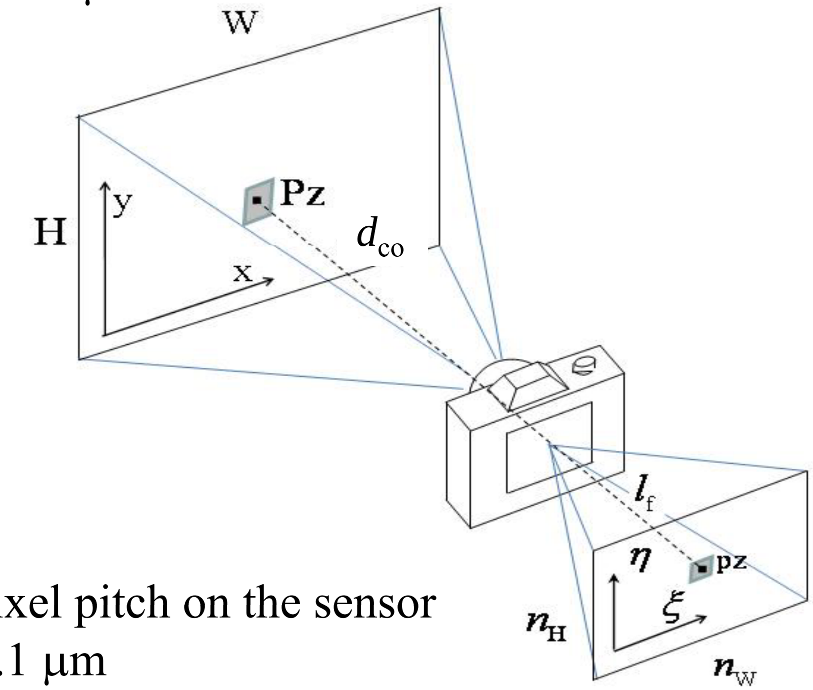

1 pixel pitch on the sensor = 6.1 μm

image space

Benchmarking

RMSE=15.9 μm (0.19 Pz)

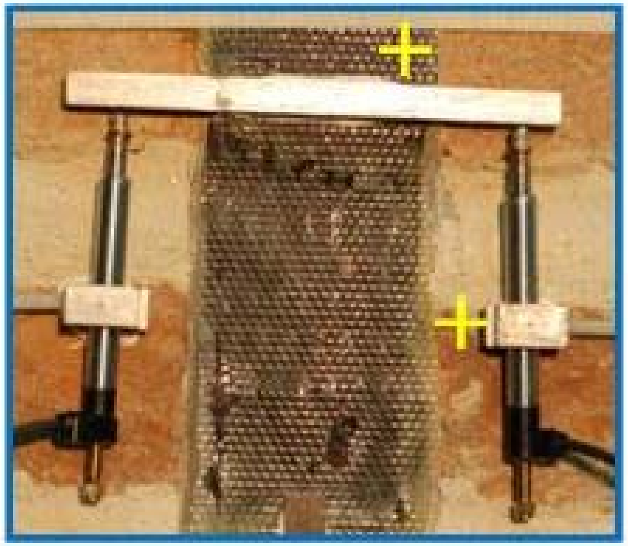

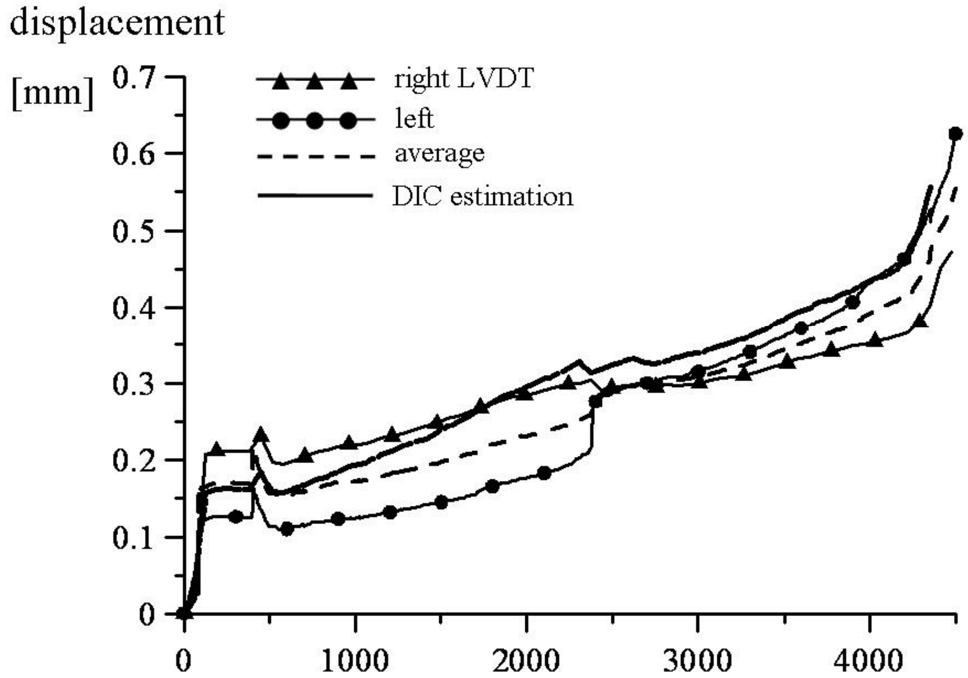
displacement
[mm]
0.7
0.6
0.5
0.4
0.3
0.2
0.1
0
right LVDT
left
average
DIC estimation
0
1000
2000
3000
4000

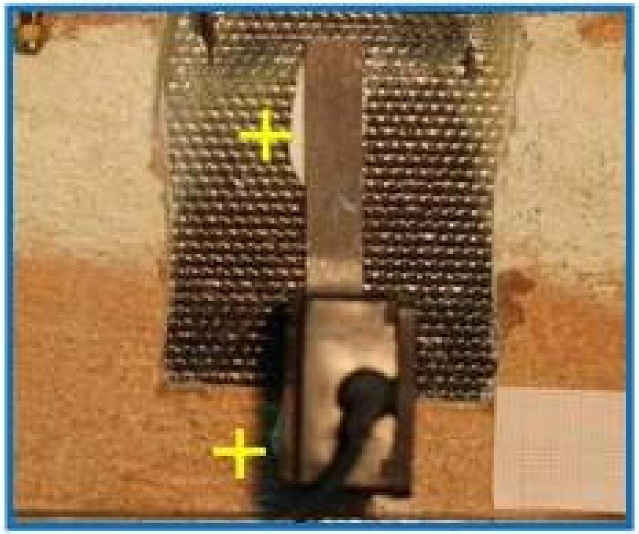

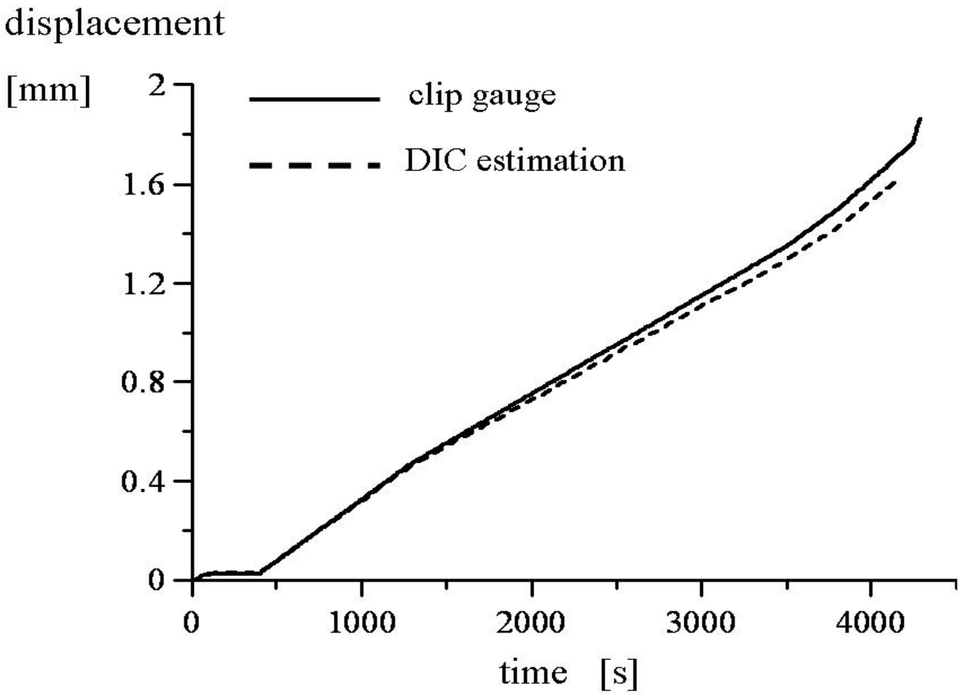
displacement
[mm]
2
1.6
1.2
0.8
0.4
0
clip gauge
DIC estimation
0
1000
2000
3000
4000
time [s]

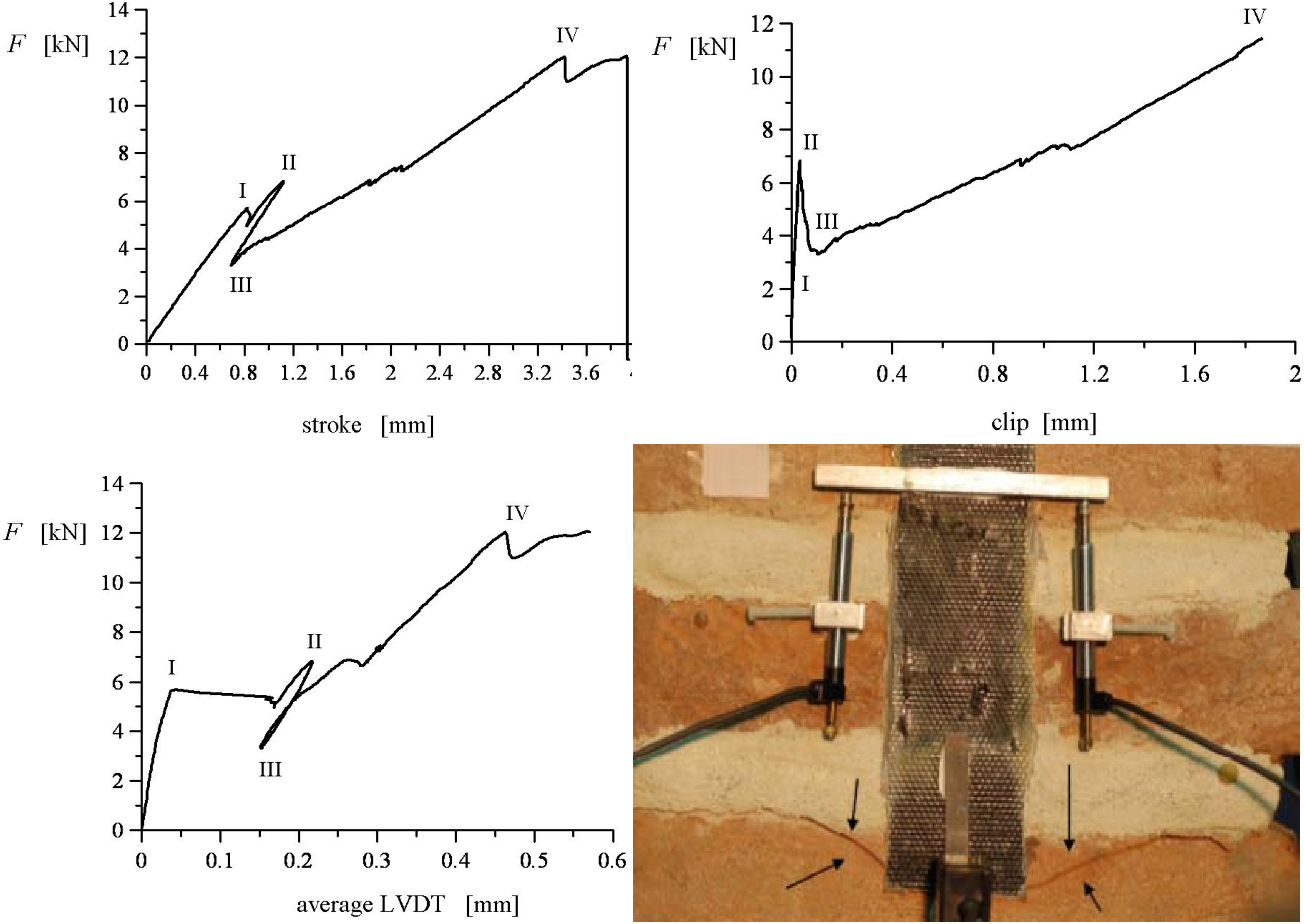

F [kN]
stroke [mm]
I
II
III
IV
F [kN]
clip [mm]
I
II
III
IV
F [kN]
average LVDT [mm]
I
II
III
IV

3D heterogeneous finite element modelling

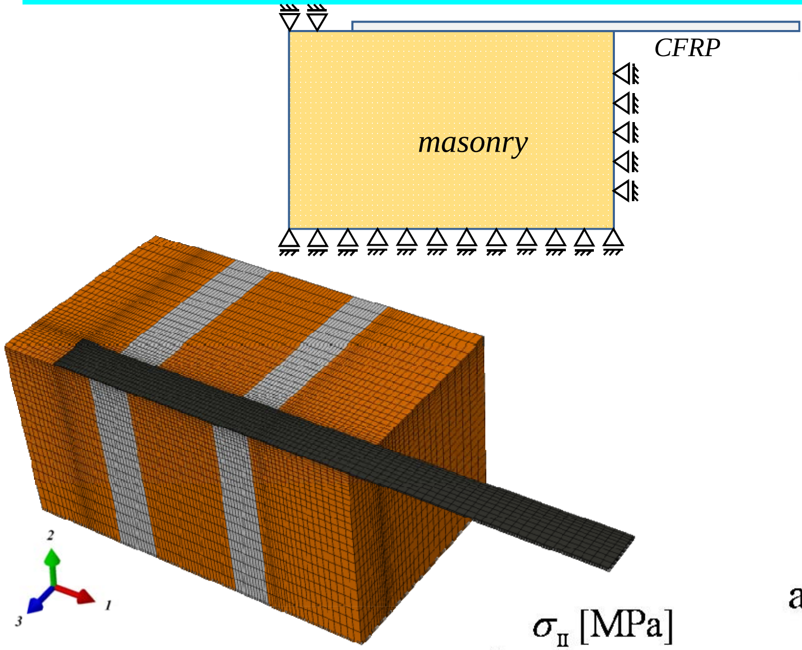

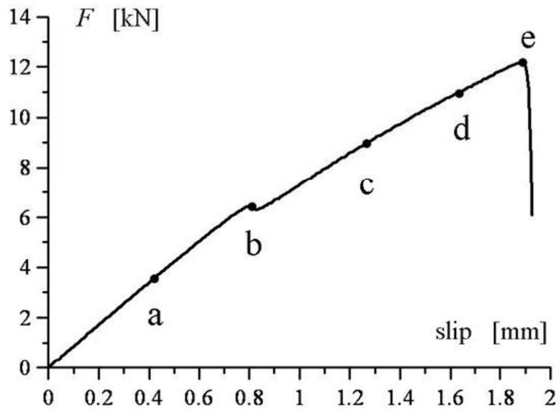

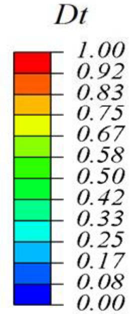

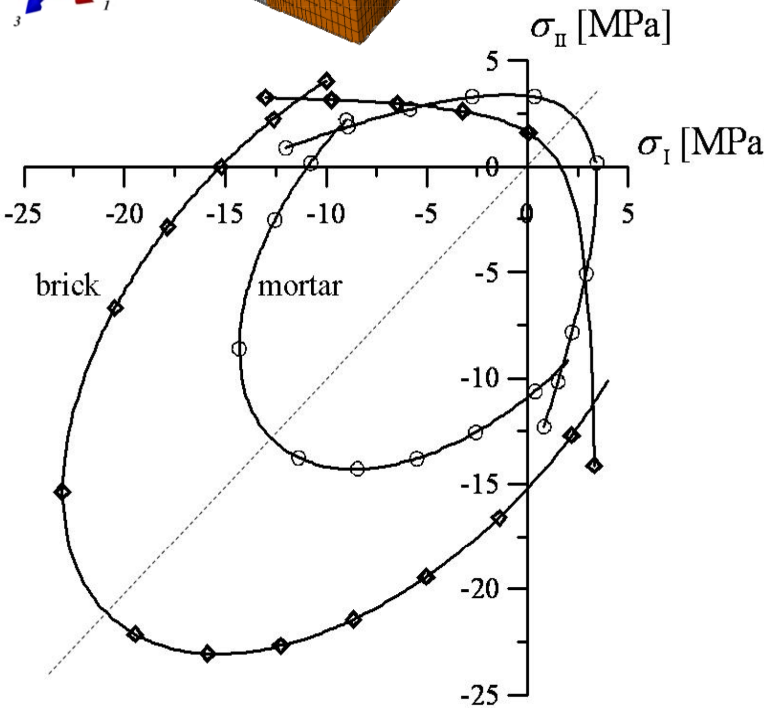

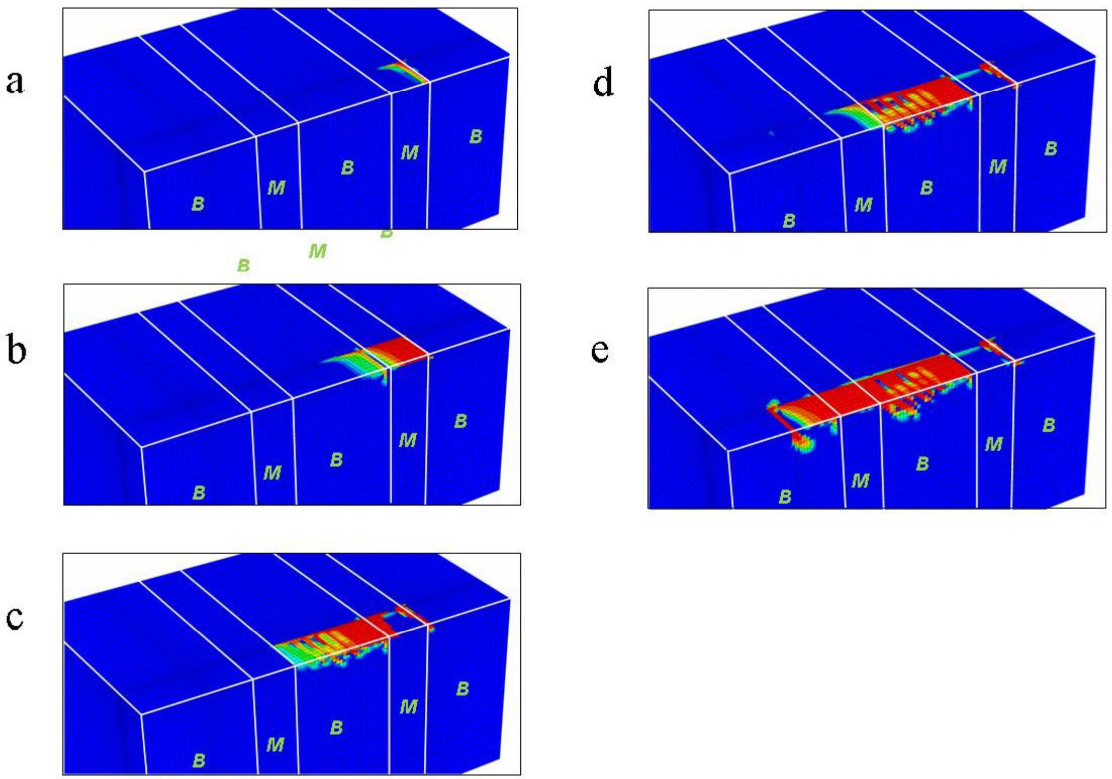

Elastic-damageable model (Comi-Perego 2001)

“bi-dissipative” model

Vumat (Abaqus© explicit)

two isotropic damage variables:

in tension D_t in compression D_c

state equations

$$\sigma_{ij} = \underbrace{(1 - D_t)\cdot(1 - D_c)}_{(1 - D)}\left[\left(K - \tfrac{2}{3}G\right)\varepsilon_v\,\delta_{ij} + 2G\,\varepsilon_{ij}\right]$$

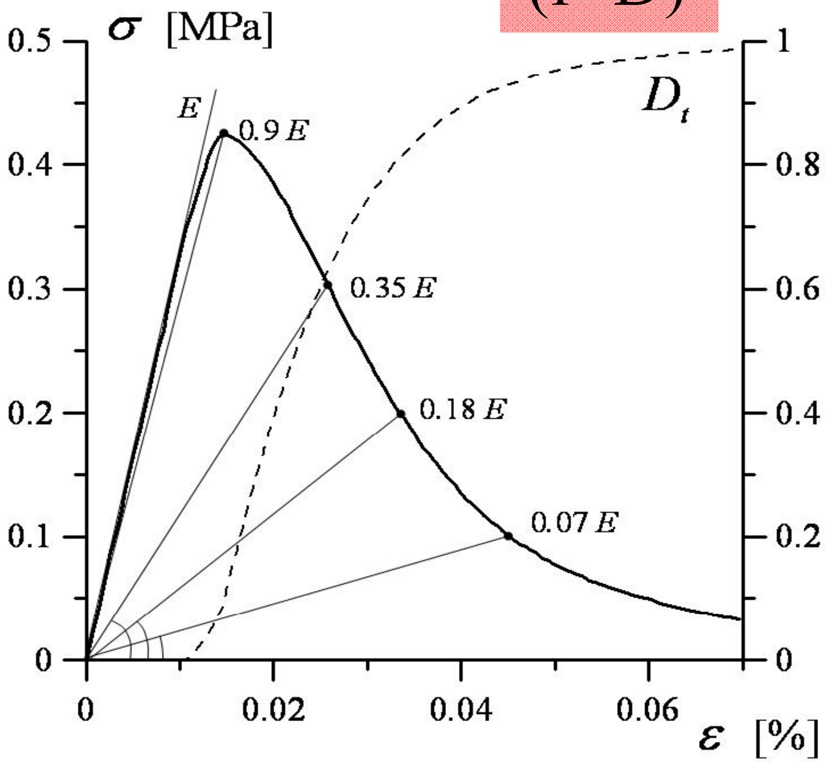

loading-unloading conditions

$$f_t(\sigma_{ij}, D_t) \le 0$$

$$\dot{D}_t \ge 0 \quad f_t\,\dot{D}_t = 0$$

$$f_c(\sigma_{ij}, D_c) \le 0$$

$$\dot{D}_c \ge 0 \quad f_c\,\dot{D}_t = 0$$

3D FE modelling with perfect adhesion

Effective elastic modulus of the CFRP reinforcement estimated by DIC

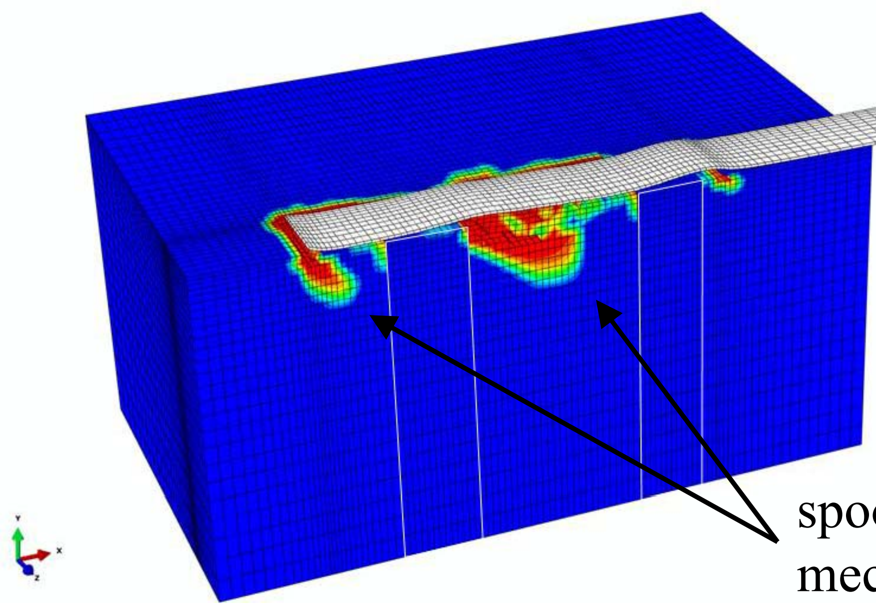

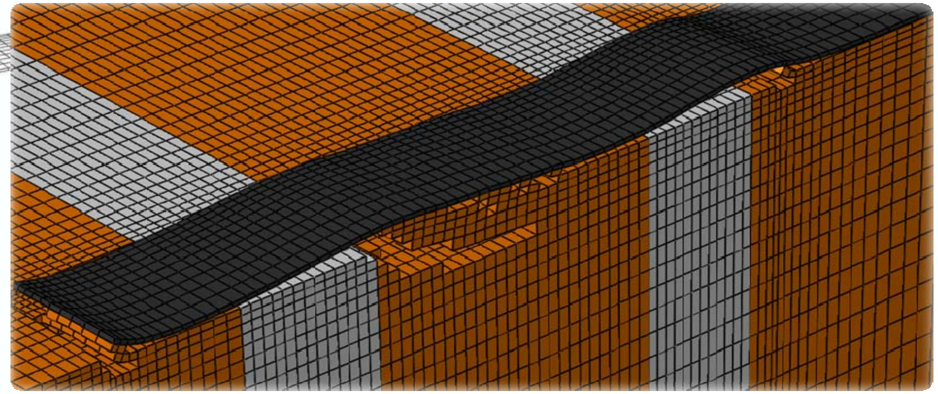

spoon shaped mechanisms

Overall delamination response

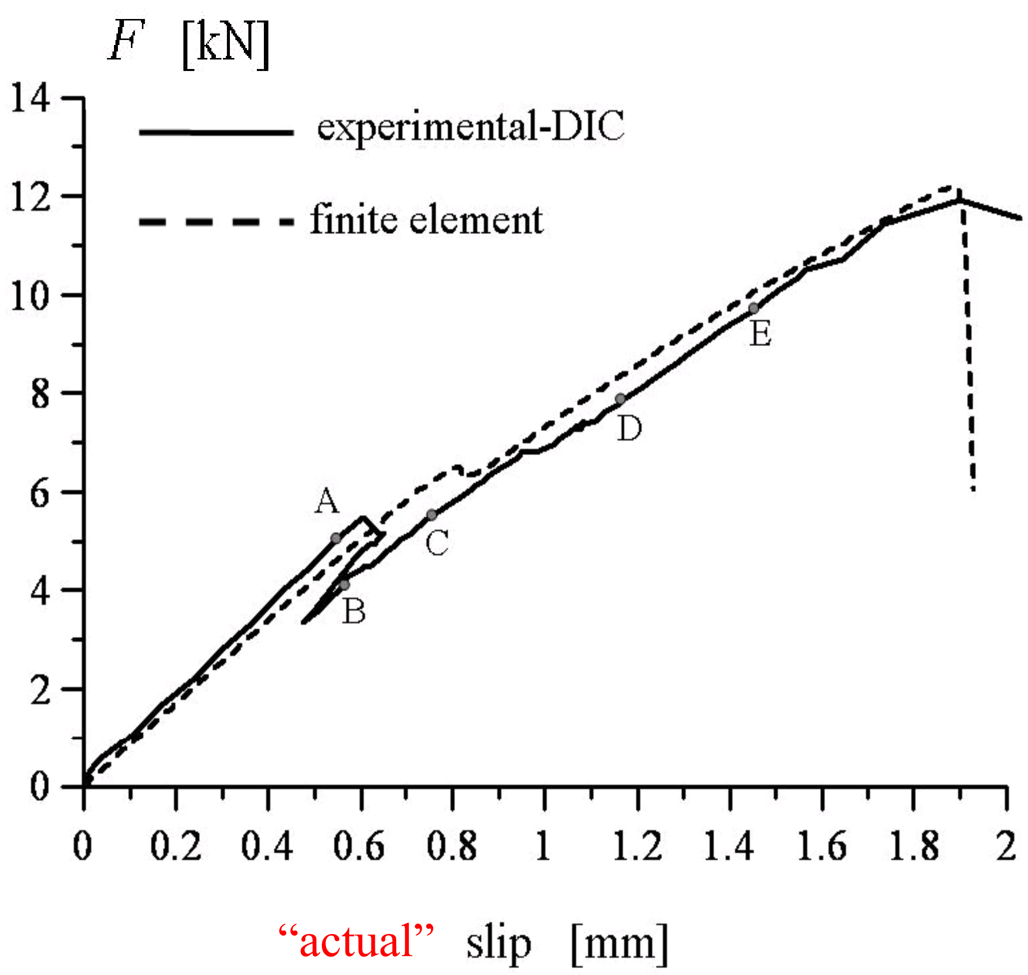

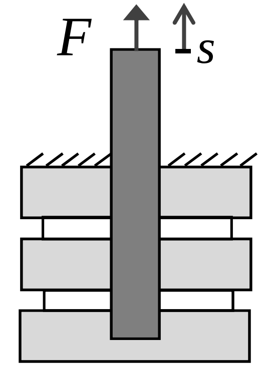

FE model with
"ideal"constraints

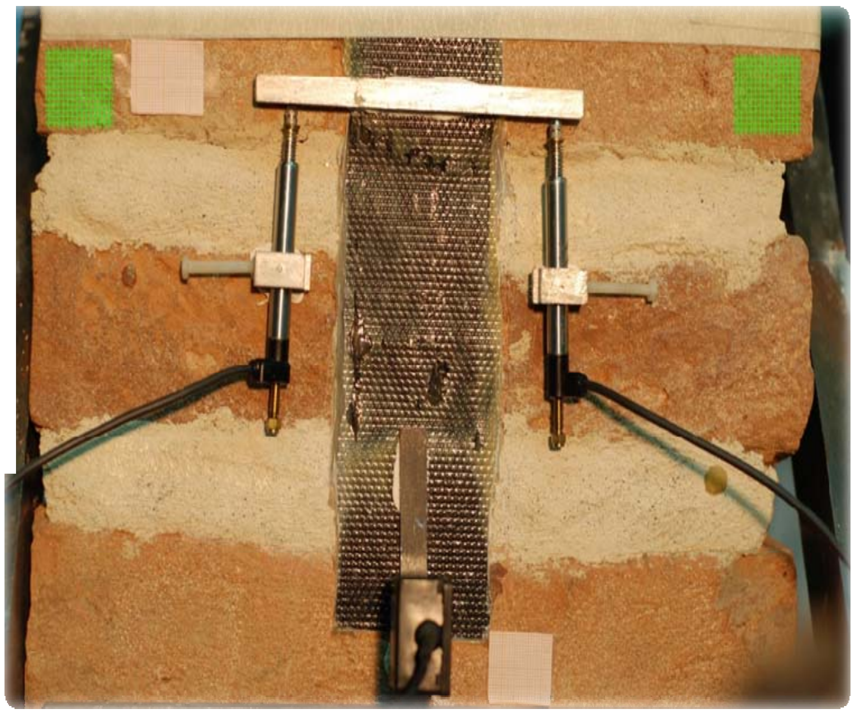

DIC-corrected boundary conditions

Local slip between FRP and masonry support

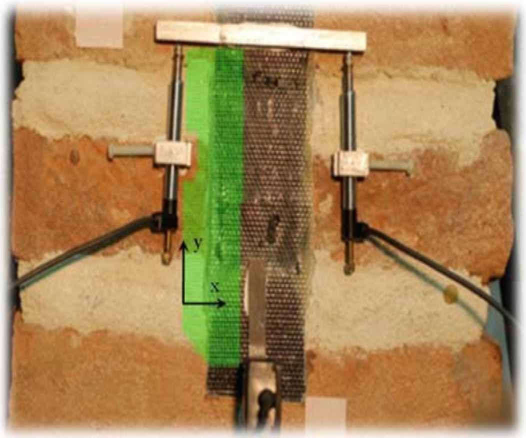

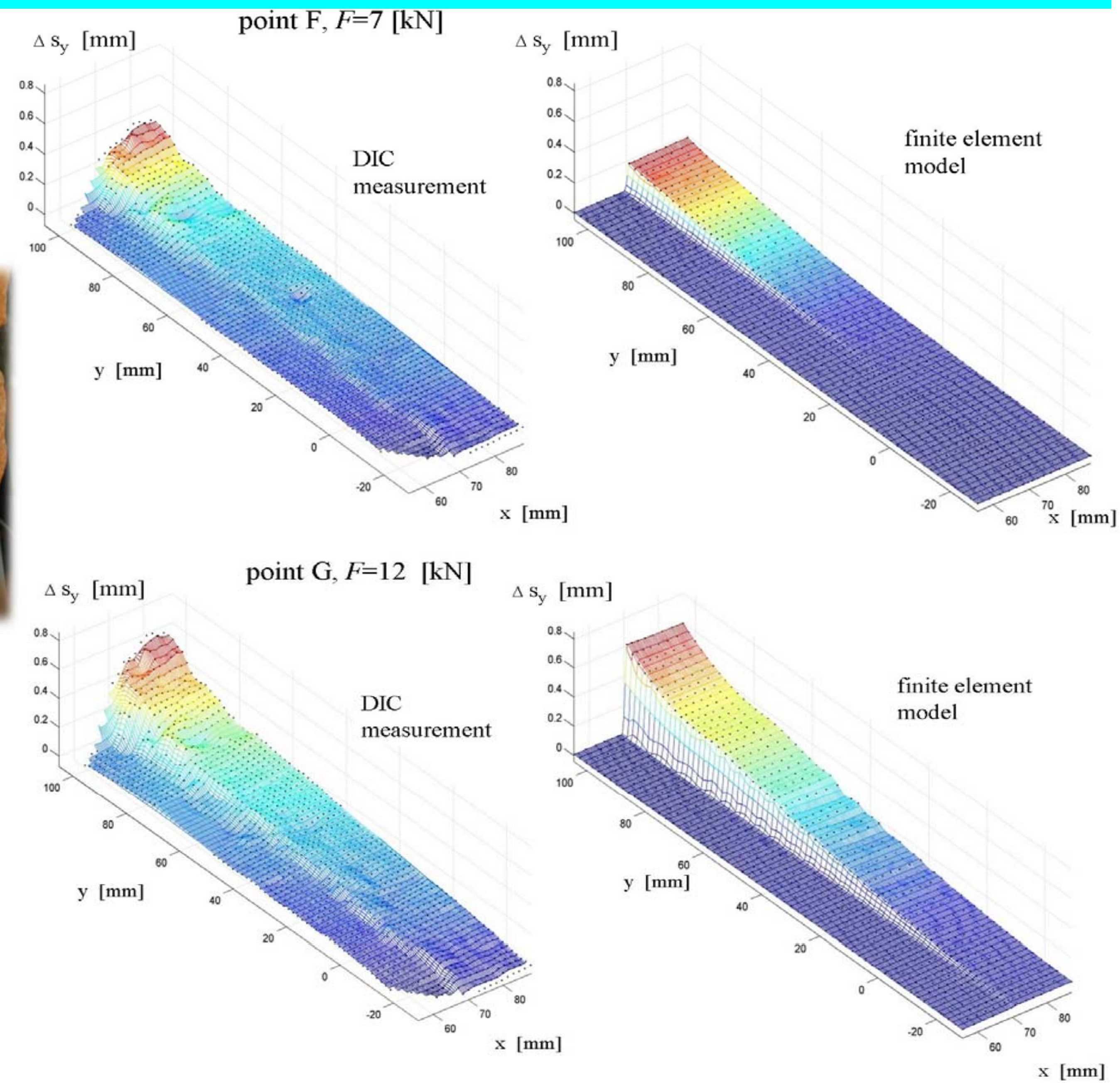

Characterization of innovative CFC/Cu joints by full-field measurements and finite elements

Roberto Fedele*, Valentina Casalegno#, Monica Ferraris#

Ref: Fedele et alii, Materials Science & Engineering A, 595 (2014) 306–317.

*Dept. of Civil and Environmental Engineering (DICA)
Politecnico di Milano, Milan, Italy

Dept of Applied Science and Technology (DISAT)
Politecnico di Torino, Turin, Italy

Composites for aggressive environments

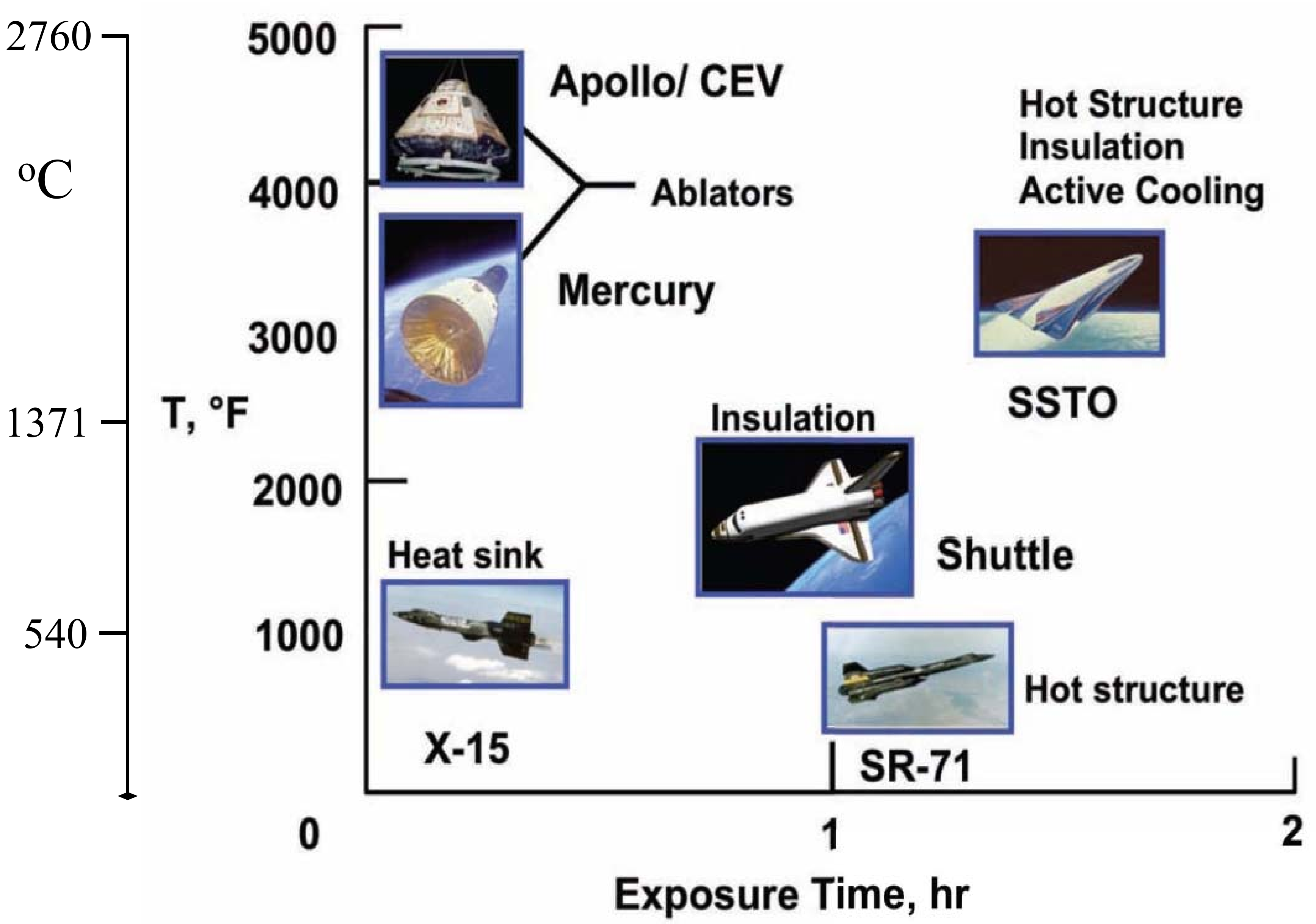

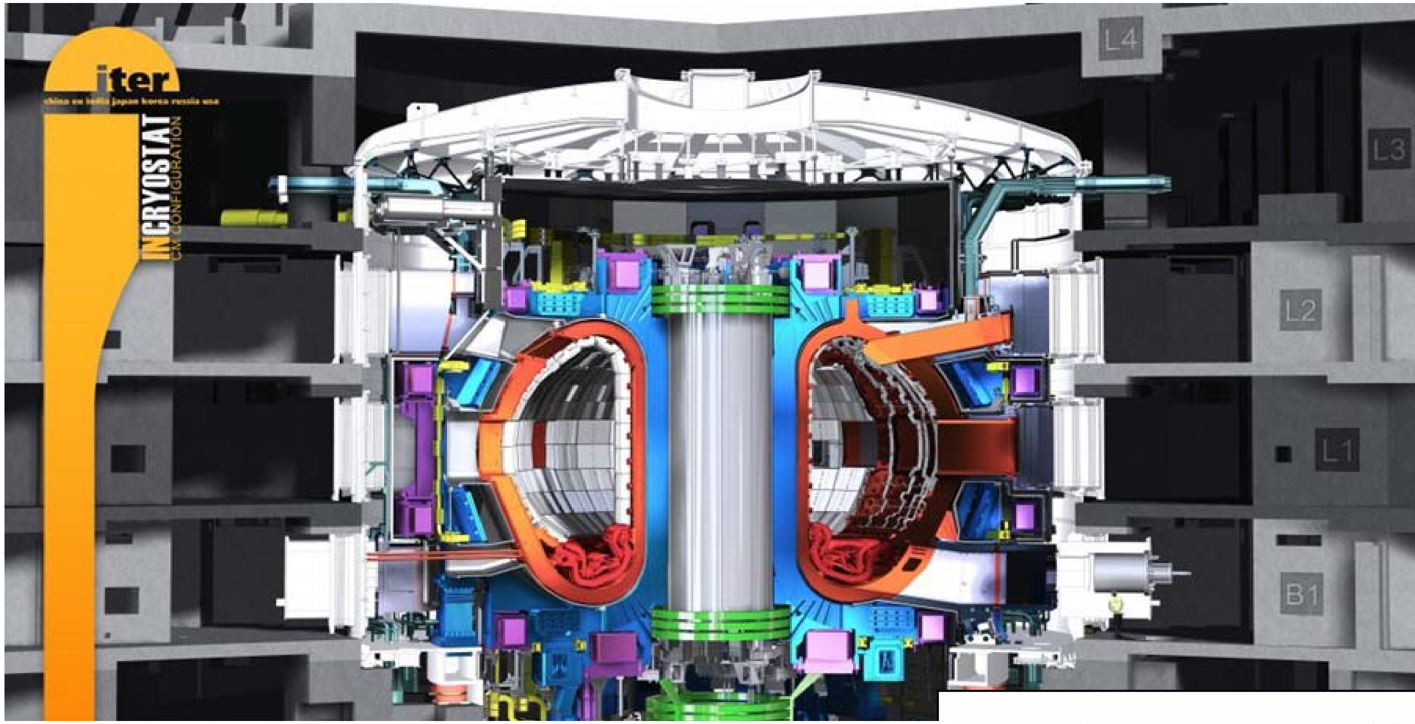

ITER
(International Thermonuclear Experimental Reactor)

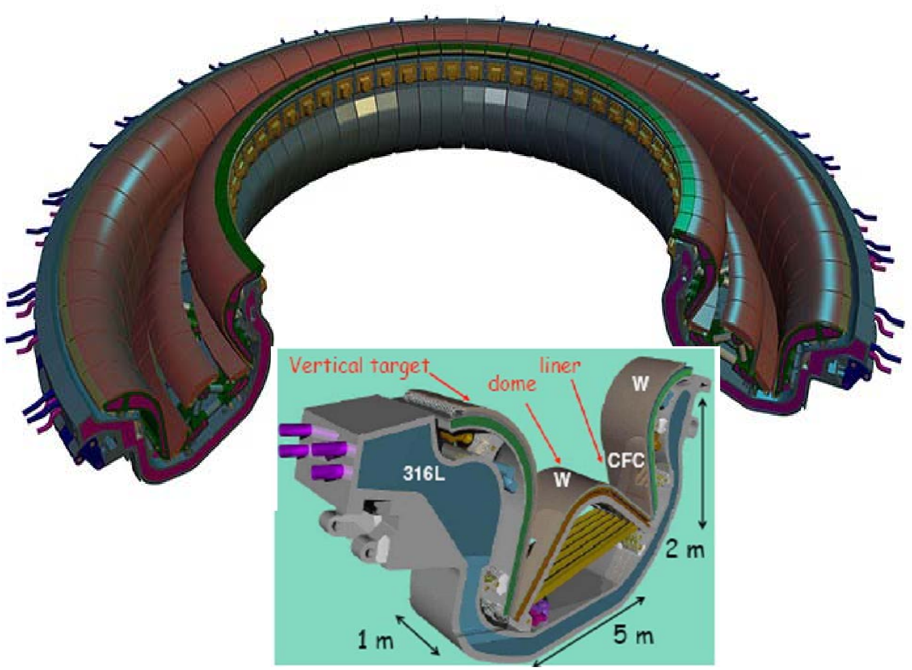

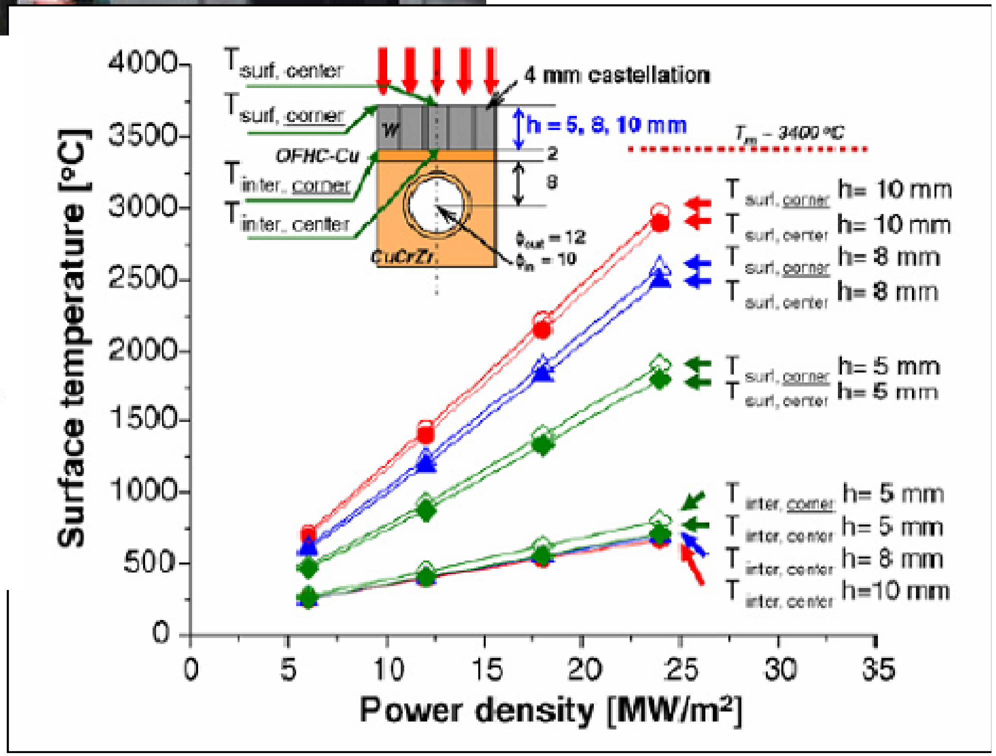

brake discs

turbine engine blades

Single-lap shear tests on flat-tile joined samples

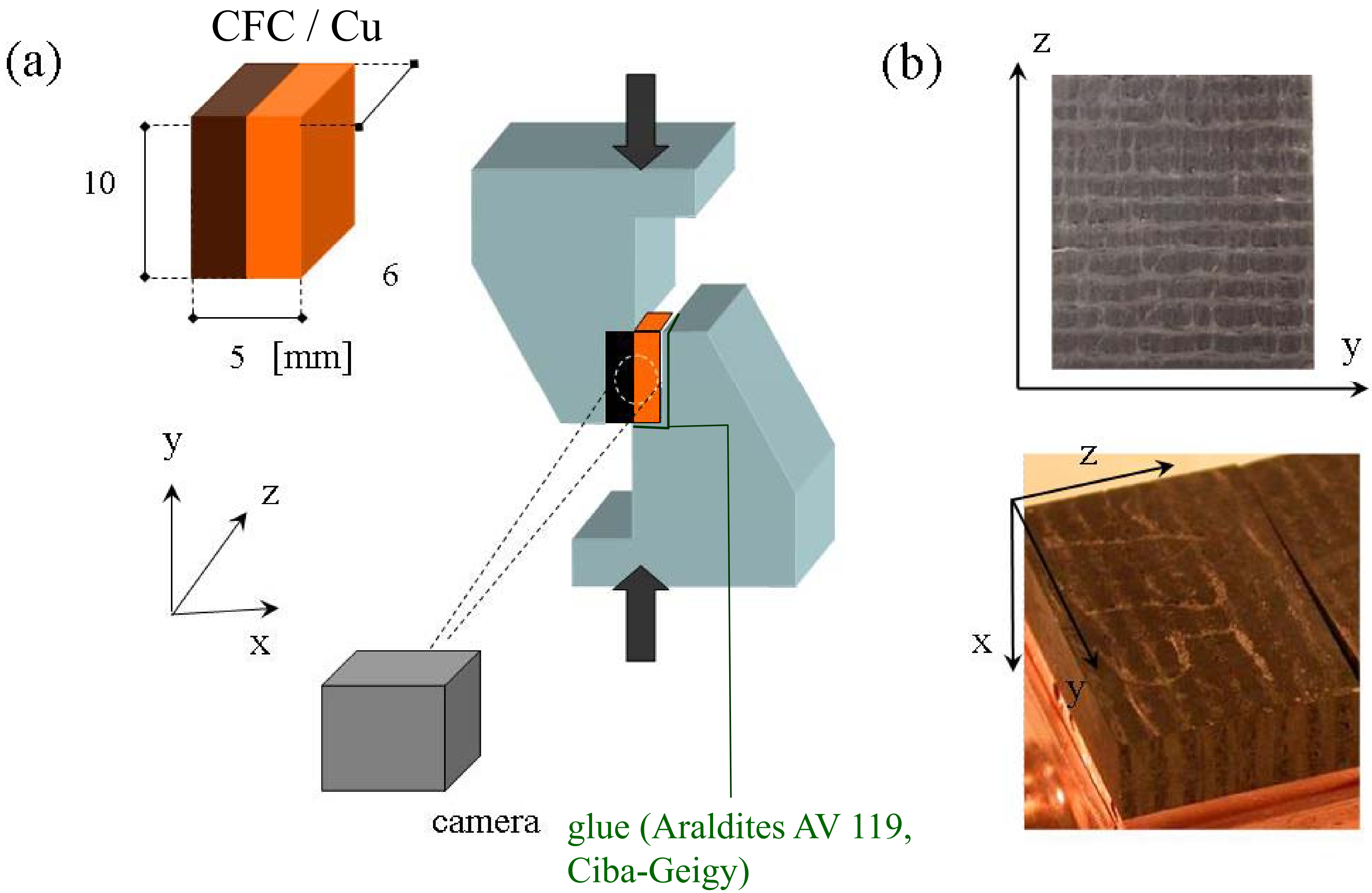

Macroscopic response

intrinsic CFC shear strength 15-20 MPa !

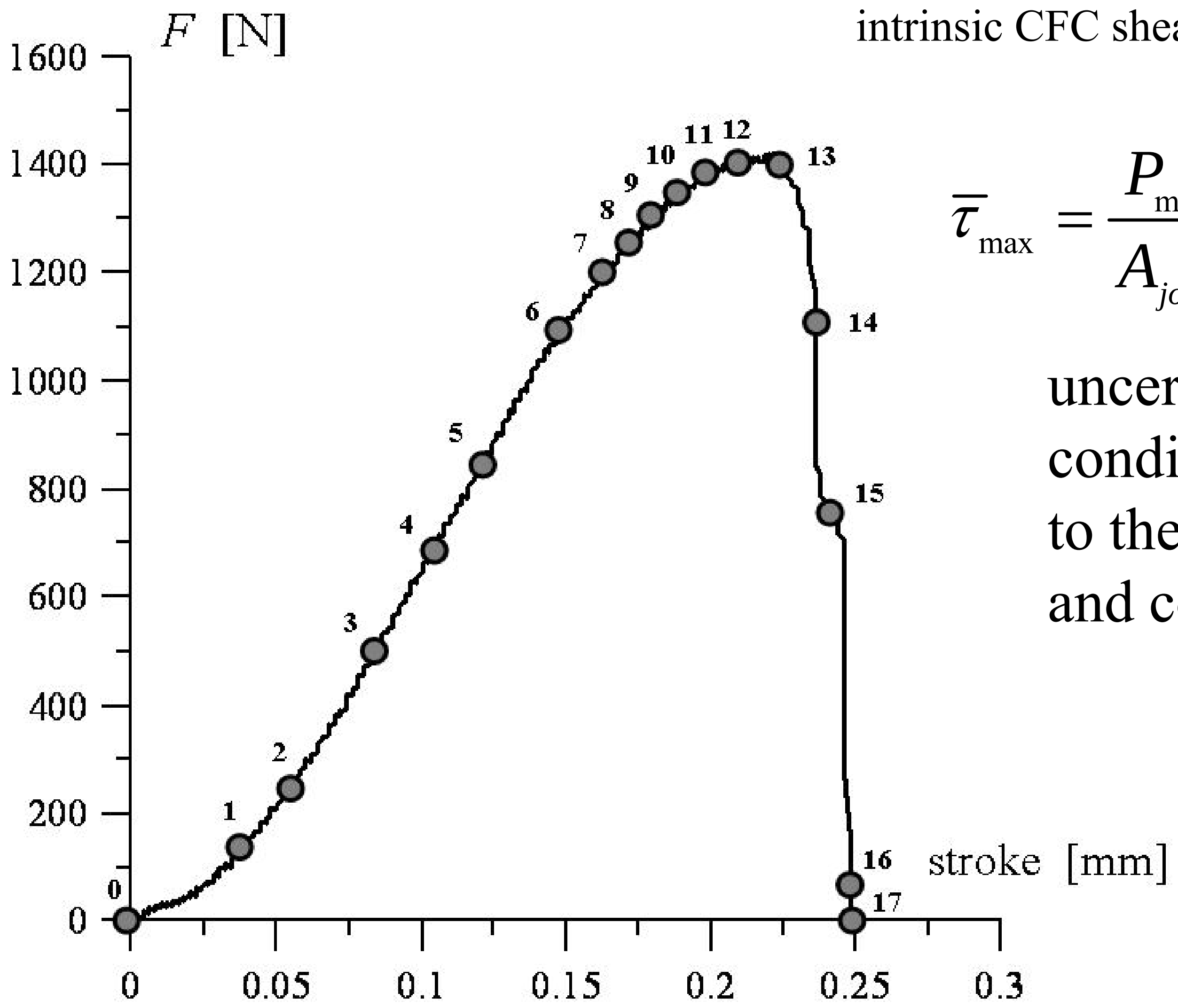

$$\overline{\tau}_{\max} = \frac{P_{\max}}{A_{joint}} \cong 23.6 \text{[MPa]}$$

uncertain boundary conditions due to the glue layers and compliant grips!

comparative assessment by different tests $\overline{\tau}_{\max} = 34 \pm 4$ [MPa]

4-dofs motion for zoomed camera for optical monitoring

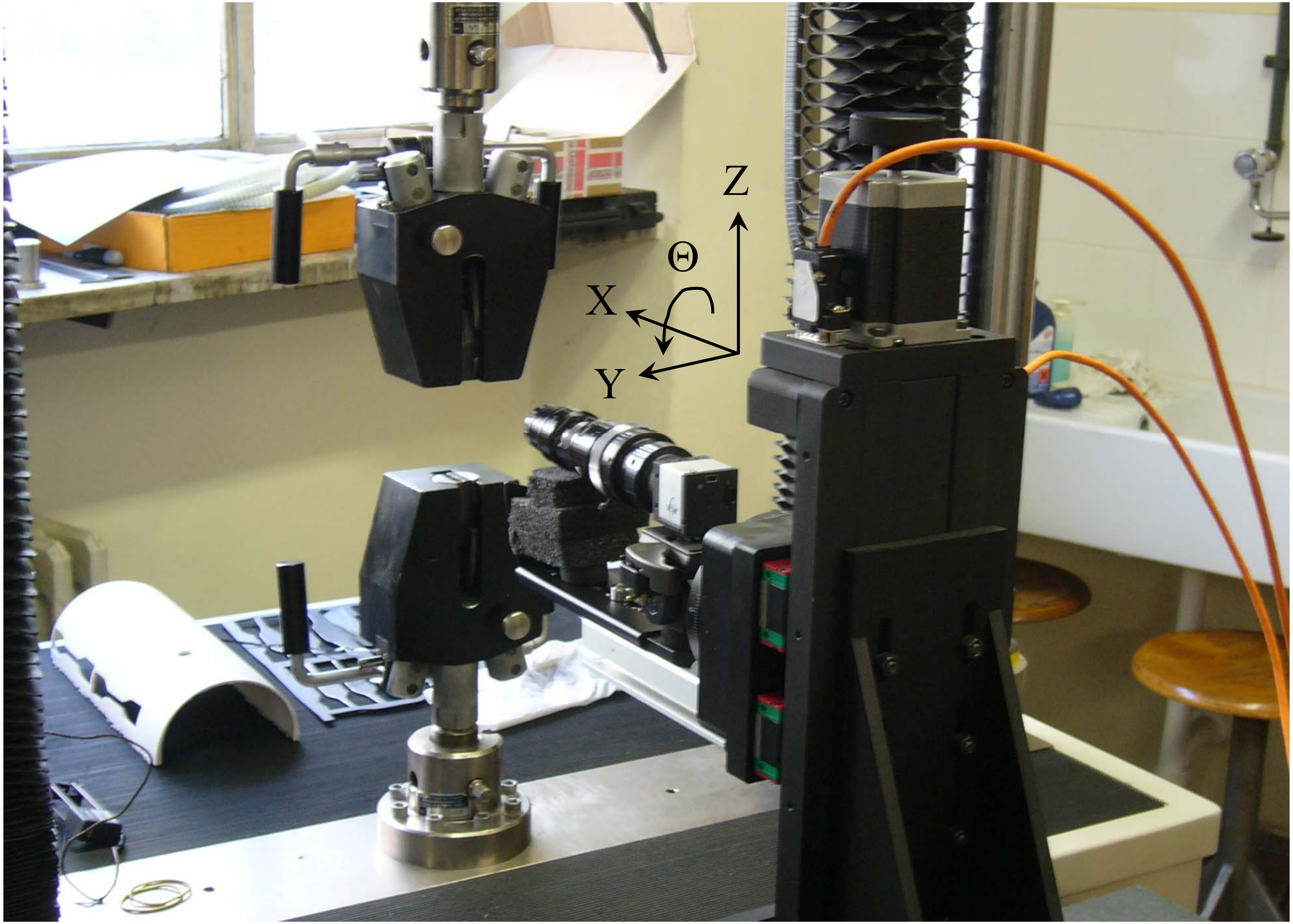

Finite element discretization of ROI

1 pixel ≅ 3.0 μm

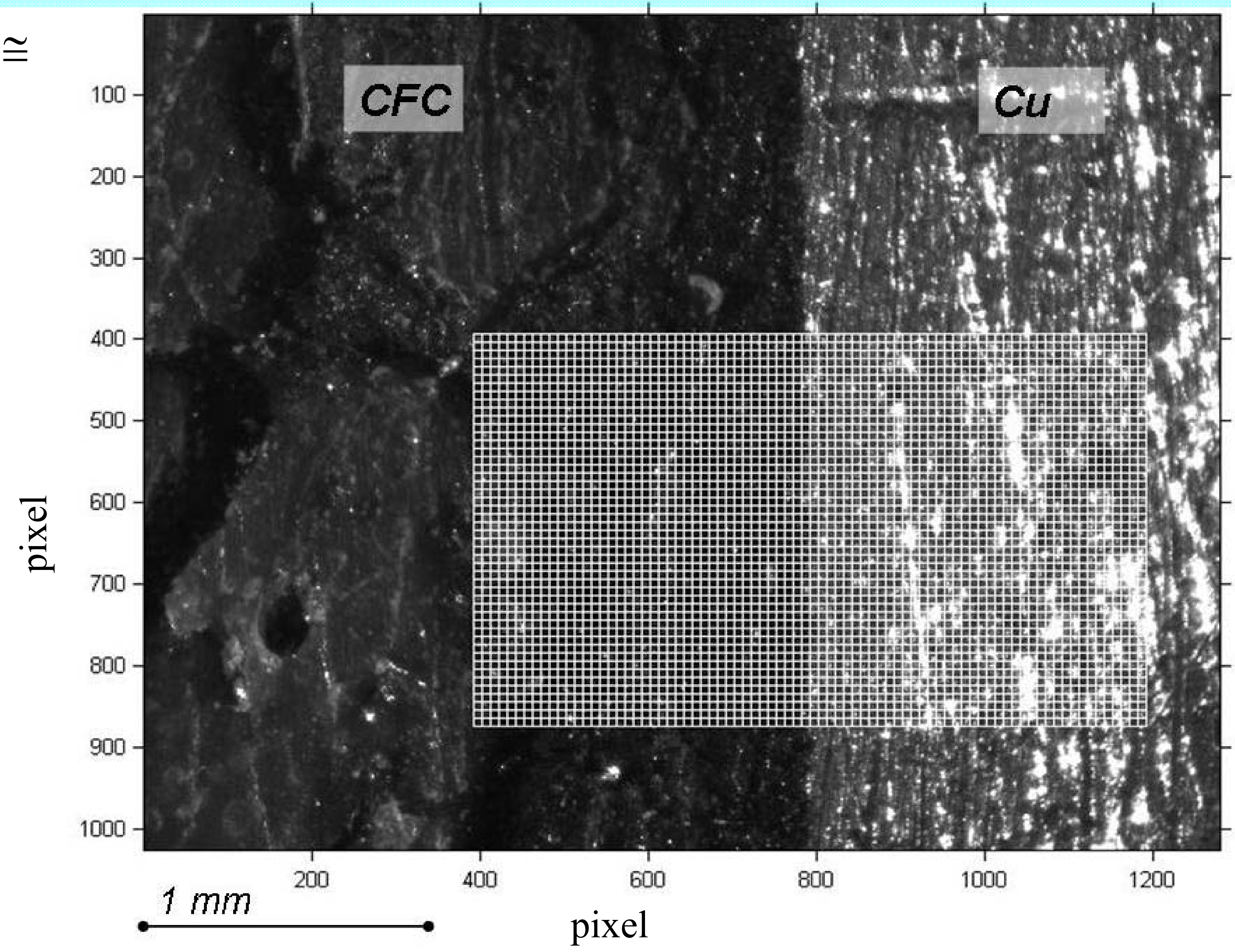

Joint collapse

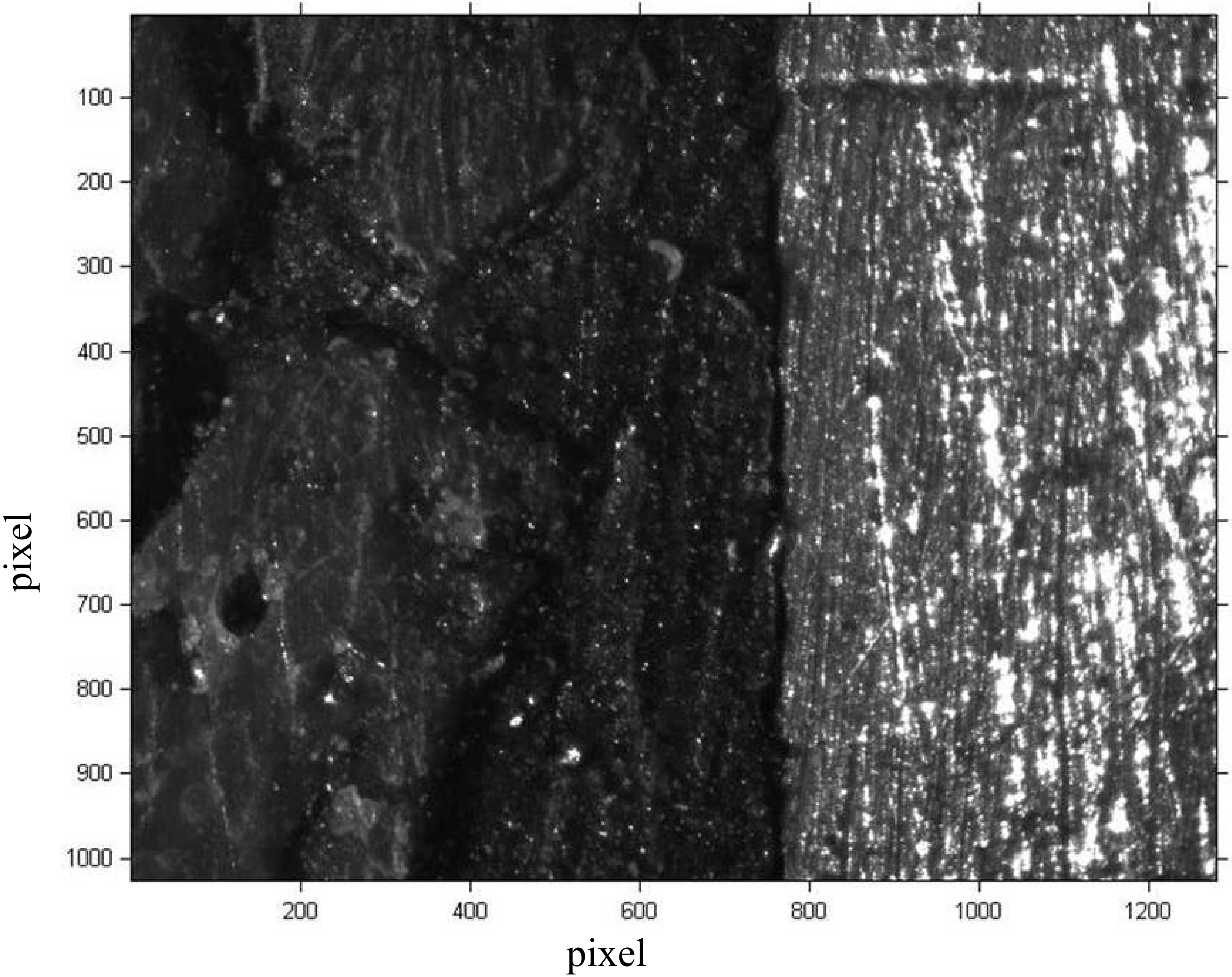

$$\bar{\Omega} = \Omega^{\circ} \cup \partial\Omega$$

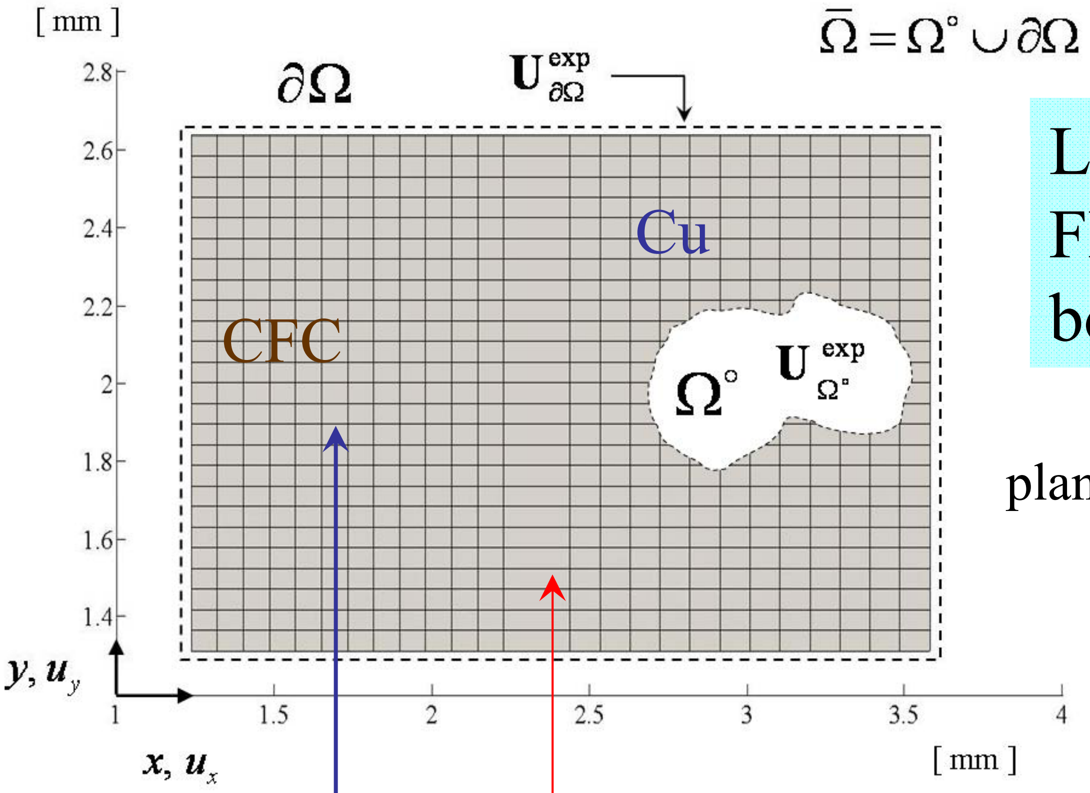

Local approach:
FE simulations driven by
boundary displacements

plane stress schematization

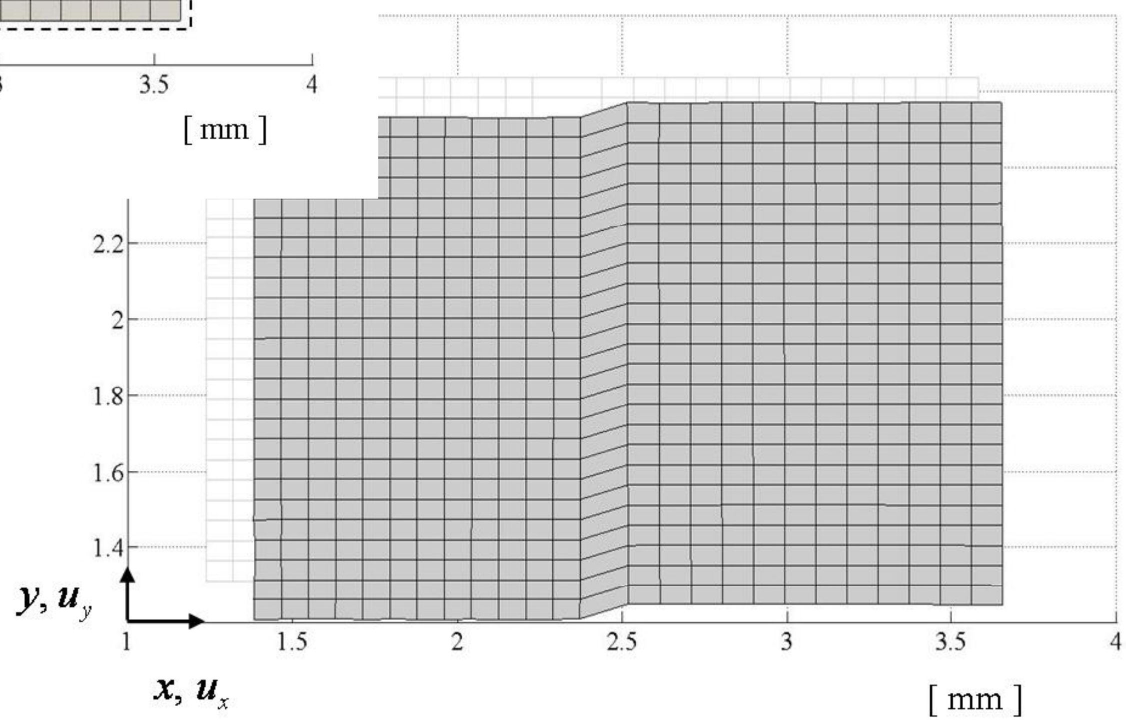

(anisotropic)
elastic-plastic
behavior

finite thickness joint

Displacement fields measured by DIC and computed

tangential component

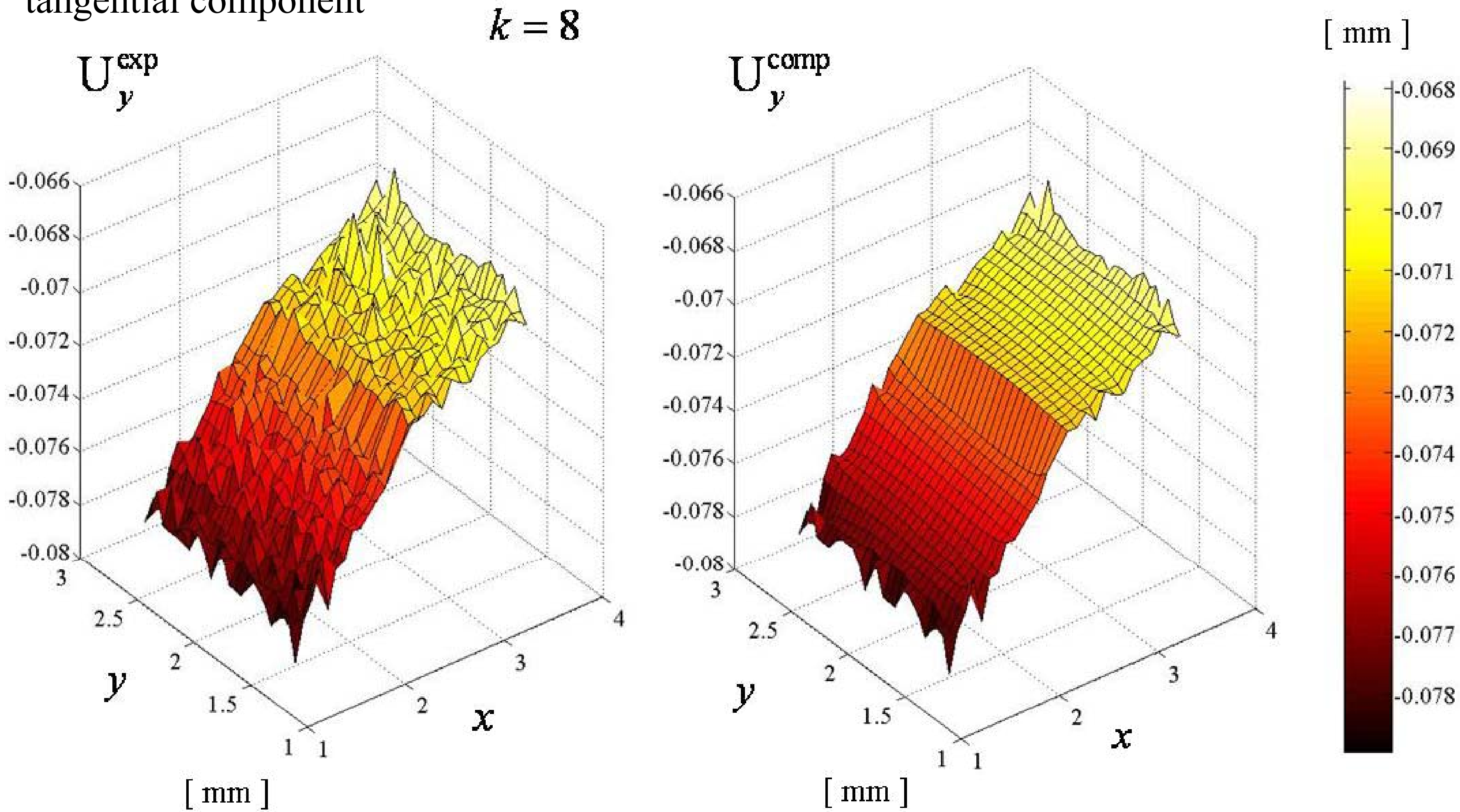

Displacement fields measured by DIC and computed

tangential component

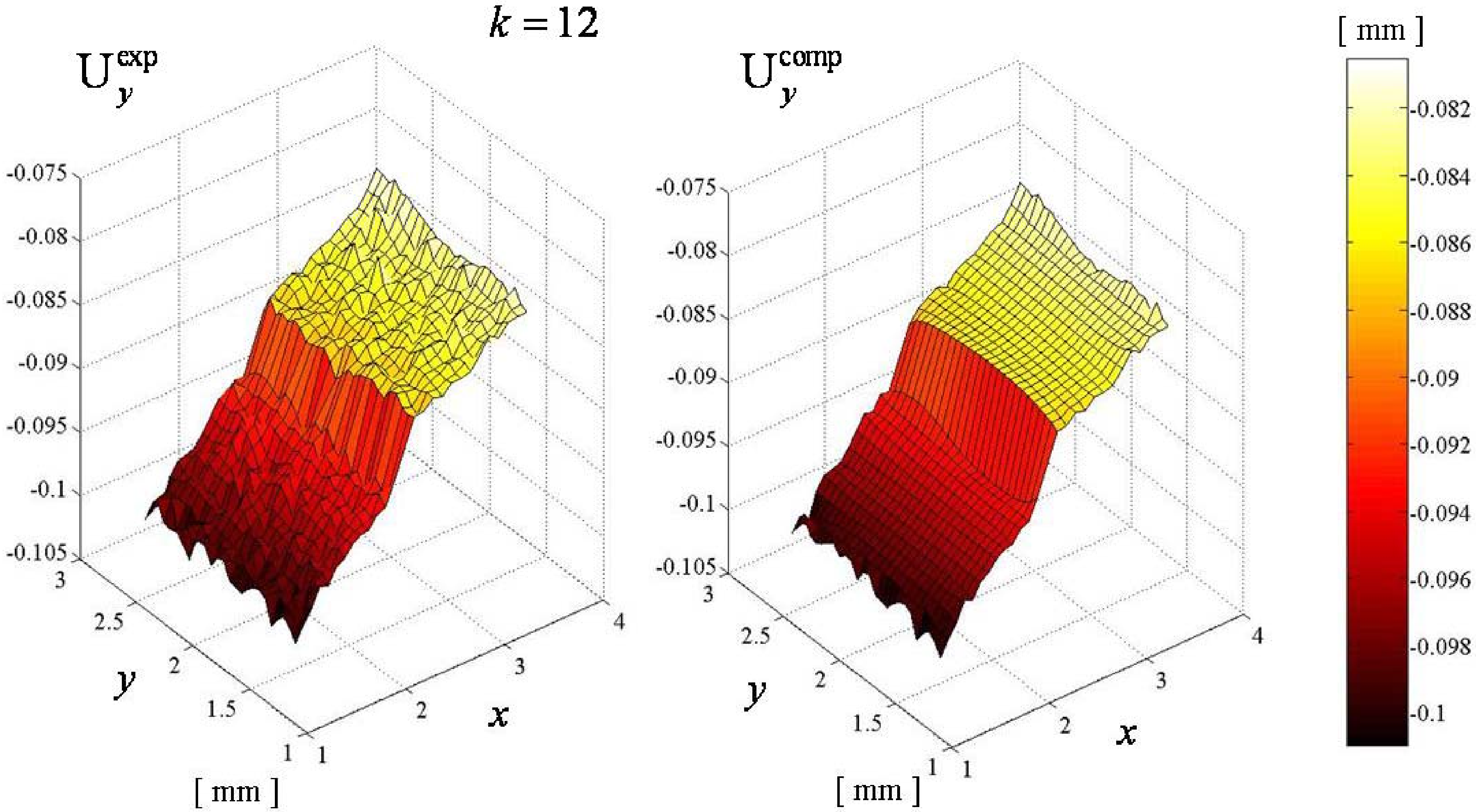

Displacement fields measured by DIC and computed

tangential component

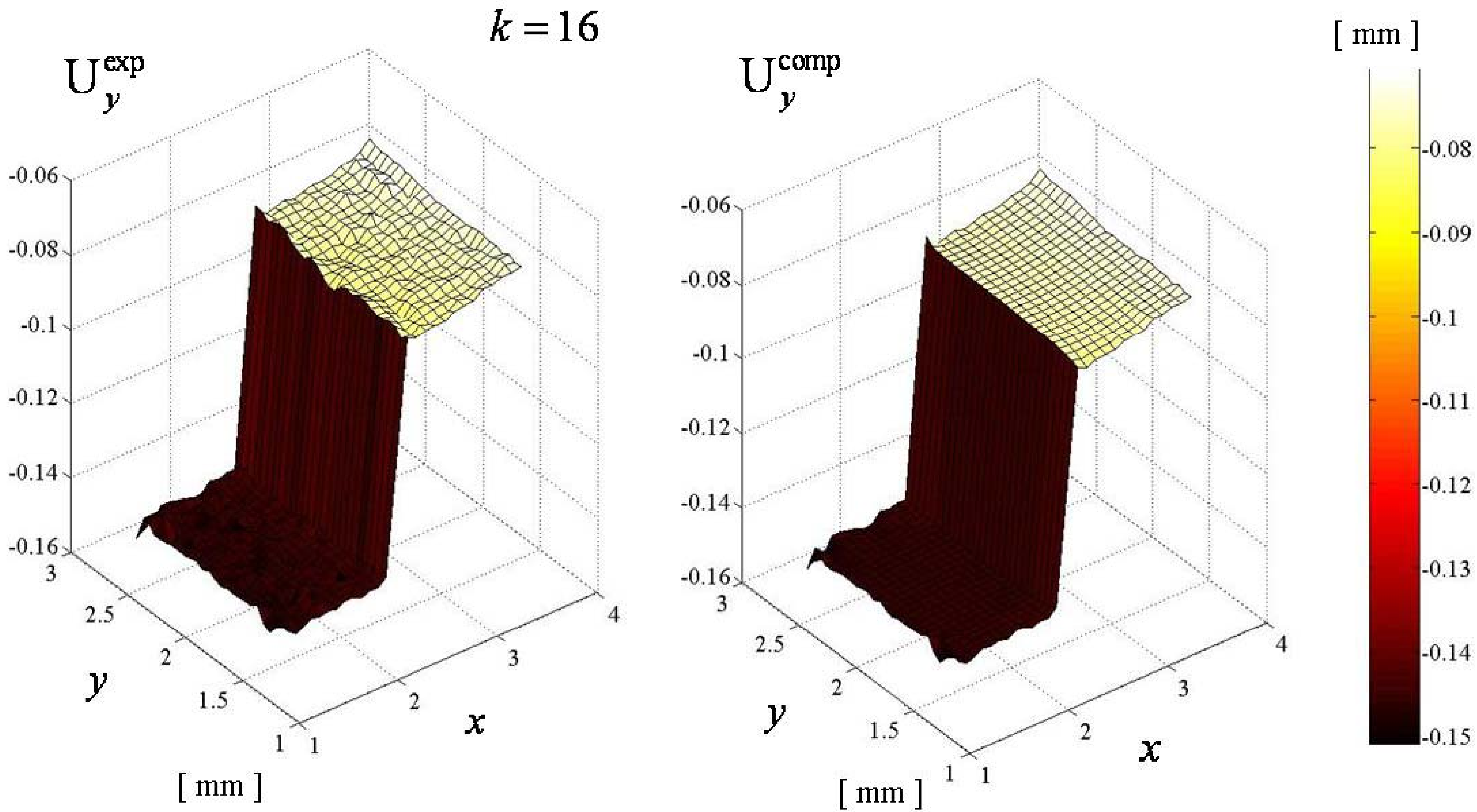

Joint governing parameters to be identified

interface tractions

"displacement jumps"

Van der Bosch, Schreurs and Geers, EFM, 2006

$$\begin{cases} p_n = \dfrac{\phi_n}{\delta_n}\left(\dfrac{\Delta_n}{\delta_n}\right)\cdot\exp\left(-\dfrac{\Delta_n}{\delta_n}\right)\cdot\exp\left(-\dfrac{\Delta_t^2}{\delta_t^2}\right) \\ p_t = \dfrac{2\,\phi_t}{\delta_t}\left(\dfrac{\Delta_t}{\delta_t}\right)\cdot\left(1+\dfrac{\Delta_n}{\delta_n}\right)\cdot\exp\left(-\dfrac{\Delta_n}{\delta_n}\right)\cdot\exp\left(-\dfrac{\Delta_t^2}{\delta_t^2}\right) \end{cases}$$

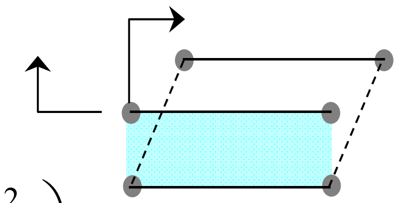

$$r = \frac{\phi_t}{\phi_n}$$

assumed a priori

parameters to identify $\mathbf{X} = \{\phi_n, \delta_n, \delta_t\}^T$

minimization
by Trust Region, reflective,
interior point Method
in a Matlab® environment

$$\hat{\mathbf{X}} = \arg\min_{\mathbf{X}} \left\{ \omega_{\mathrm{u}}(\mathbf{X}) = \sum_{k=1}^{n_t} \mathbf{R}_k^T \mathbf{R}_k \right\}$$

$$\mathbf{R}_k = \mathbf{W}_k^{-1/2} \cdot \left[\mathbf{U}_{\Omega^\circ}^{\exp\ k} - \mathbf{U}_{\Omega^\circ}^{\mathrm{comp}\ k}\left(\mathbf{X} \,\middle|\, \mathbf{U}_{\partial\Omega}^{\exp\ k}\right) \right] \quad k,\ k = 1, \ldots, n_t$$

boundary conditions provided by DIC
were deterministically prescribed without any regularization provision

Tangential stress evolution

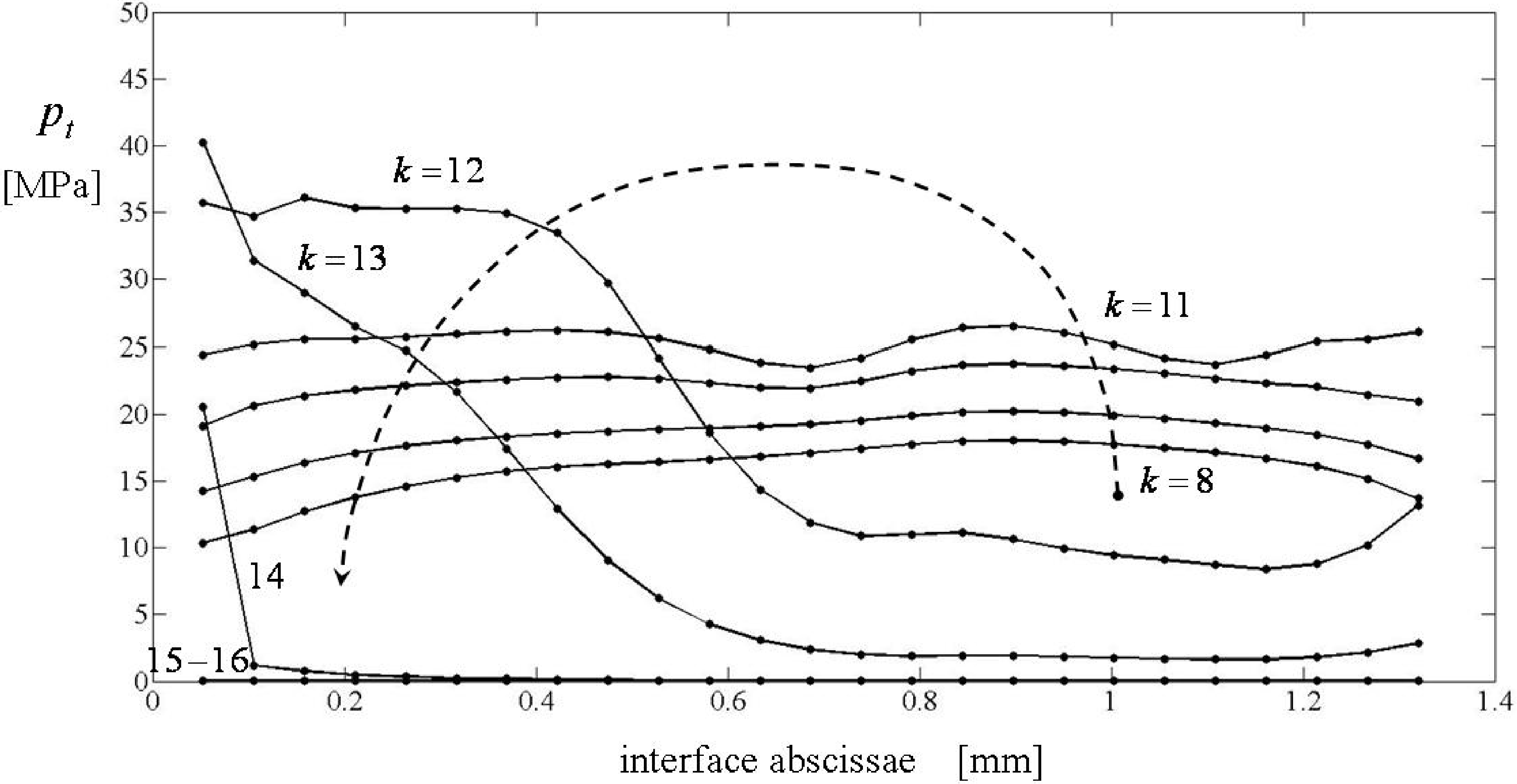

traction predicted under pure mode II

$$(p_t)_{max} \simeq 43 \text{ MPa}$$

Normal stress evolution

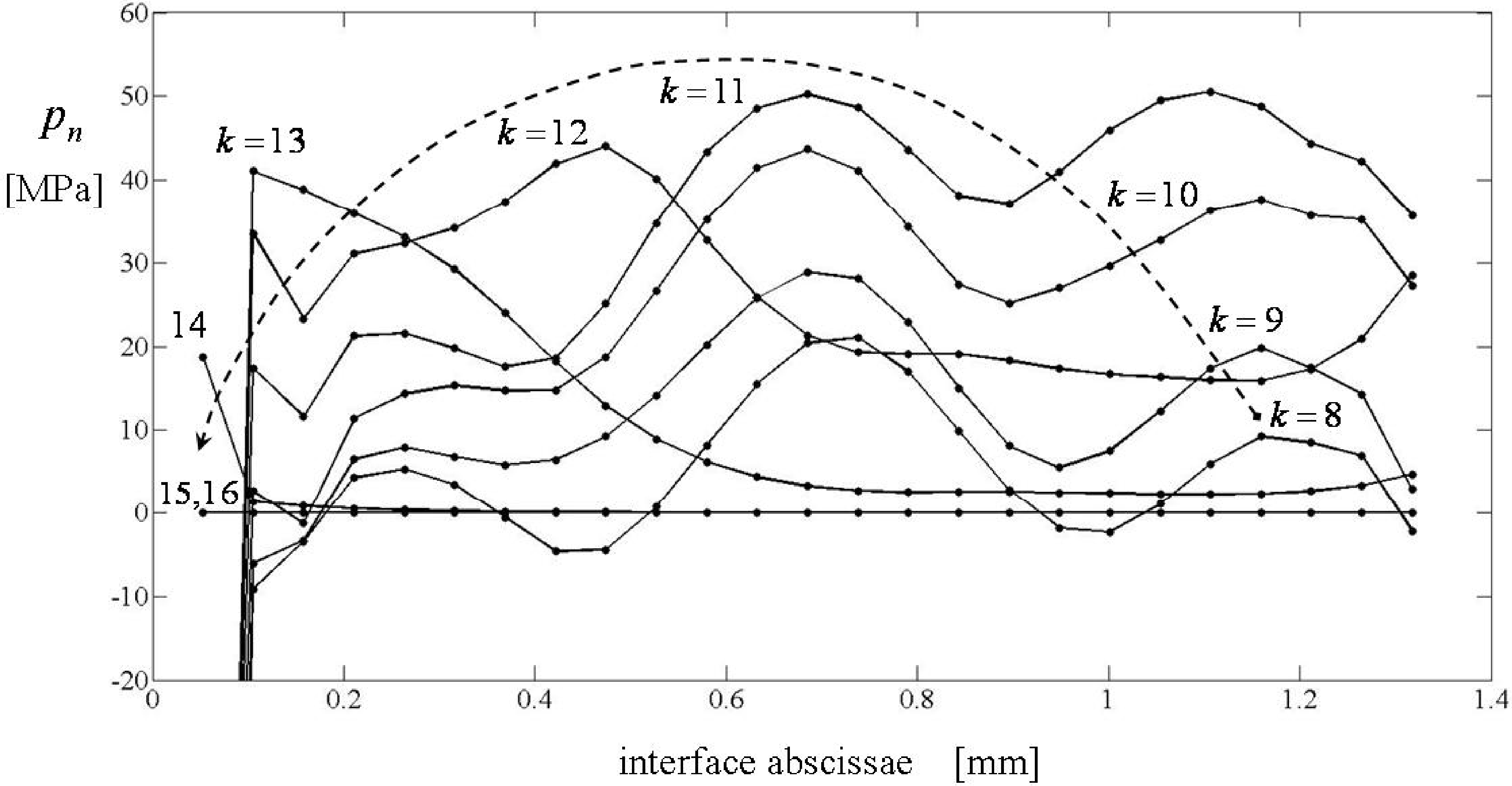

traction predicted under pure mode I

$$\left(p_n\right)_{\max} \simeq 58 \text{ MPa}$$

Closing remarks and future prospects

- DIC measurements especially suitable for calibration/validation of FE models with special reference to :
  (i) accuracy of 2D/3D geometry assumptions ;
  (ii) boundary data estimation ;
  (iii) response of joint/interfaces ;
  (iv) constitutive relationships .

- Information fusion
  from several sensors
  and diverse testing configurations

- Extension to High and Ultra High Temperature (UHT) testing (?)


095
100
F

$I_1 \equiv \mathrm{tr}\,\boldsymbol{\sigma} = \sigma_{ij}\delta_{ji}$ [MPa]
first invariant stress tensor

$J_2 \equiv \left(\frac{3}{2} S_{ij} S_{ji}\right)$ [MPa²]
second invariant stress deviator

$h_i(D_i) \quad (i = t, c)$
hardening/softening functions

meridian plane

$$f_c(\boldsymbol{\sigma}, D_c) = J_2 + a_c I_1^2 + b_c h_c I_1 - k_c h_c^2 = 0$$

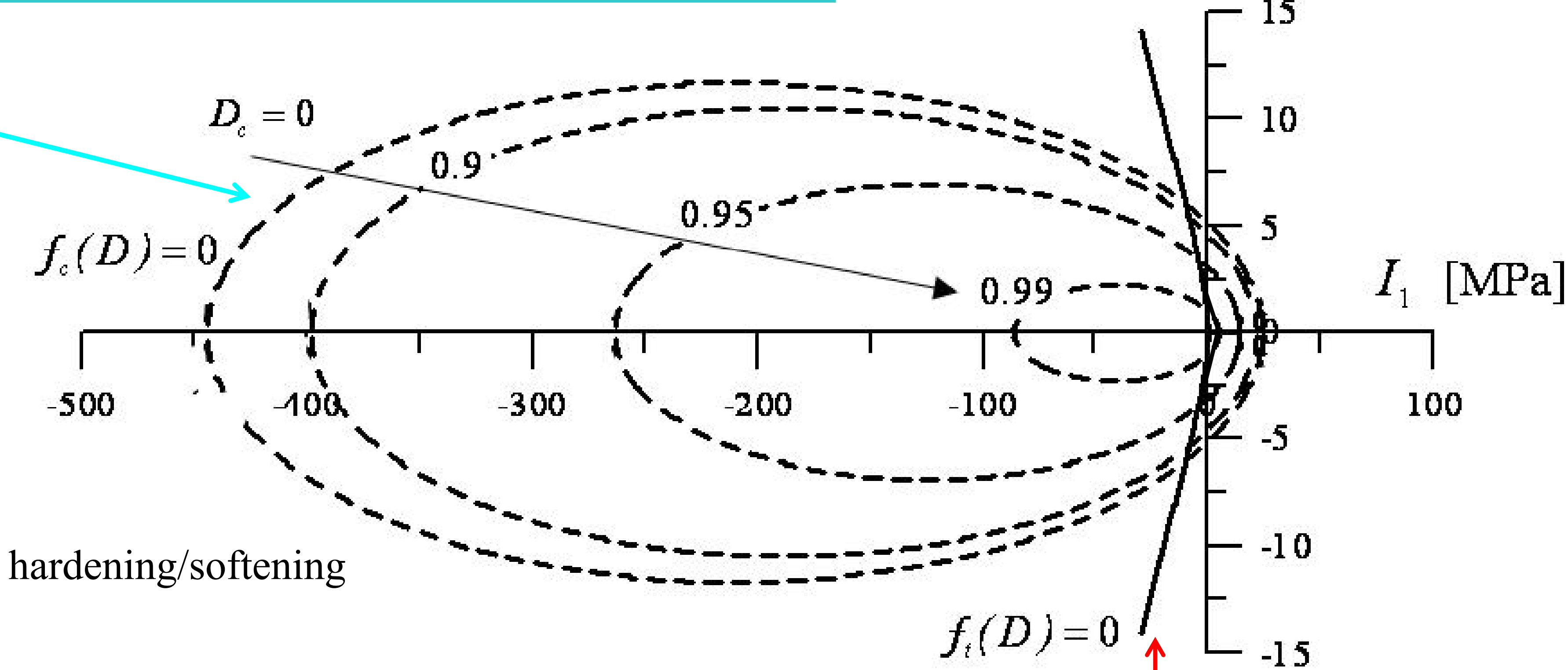

$$f_t(\boldsymbol{\sigma}, D_t) = J_2 - a_t I_1^2 + b_t h_t I_1 - k_t h_t^2 = 0$$

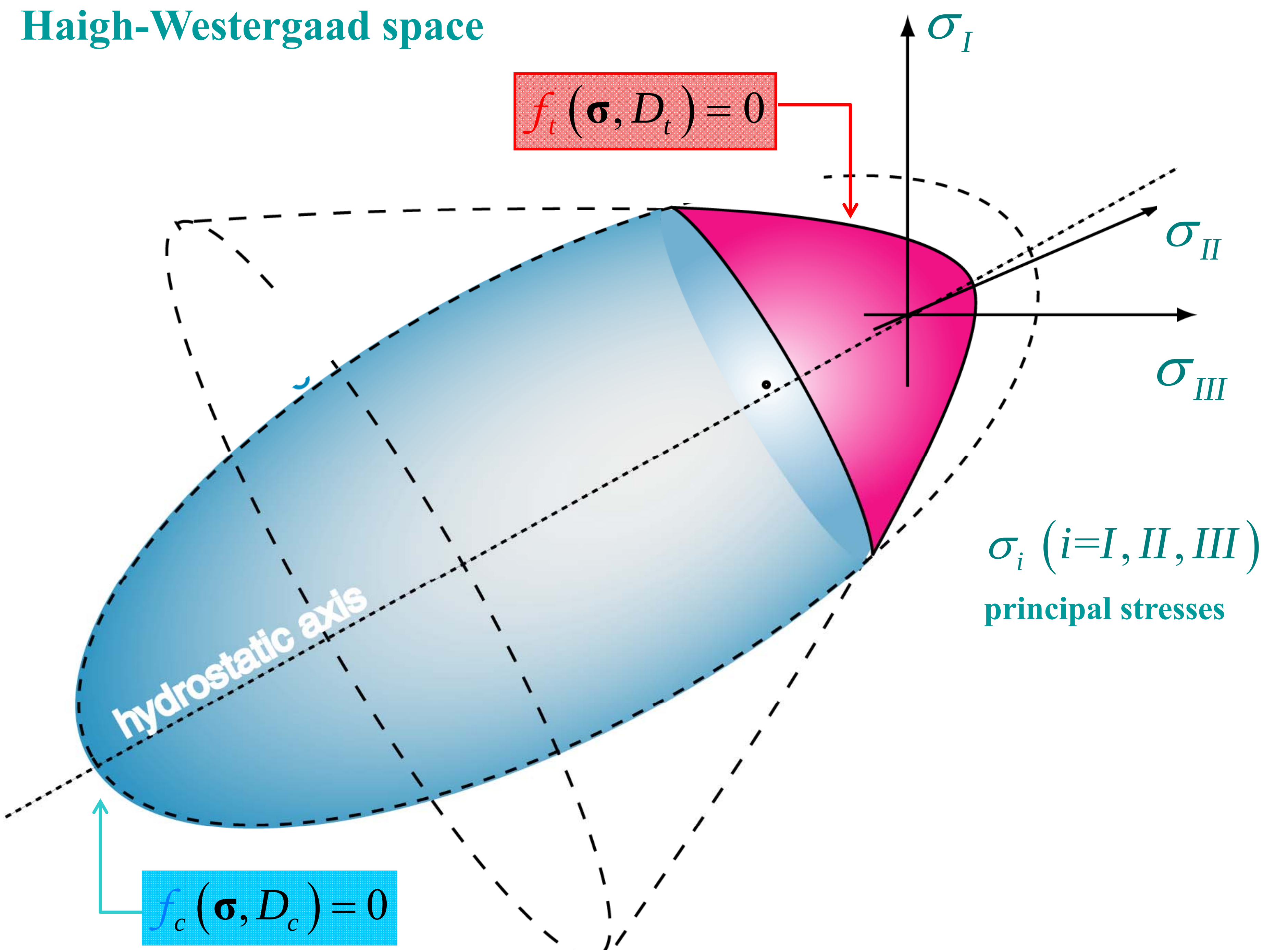

Haigh-Westergaad space
$f_t(\boldsymbol{\sigma}, D_t) = 0$
σ_I
σ_{II}
σ_{III}
hydrostatic axis
$\sigma_i \ (i = I, II, III)$
principal stresses
$f_c(\boldsymbol{\sigma}, D_c) = 0$

Fracture energy regularization

specific fracture energy

$$g_i(\mathrm{m}_i) = \frac{G_i}{l_{\mathrm{ch}}^{(\mathrm{e})}}$$

"element" characteristic length

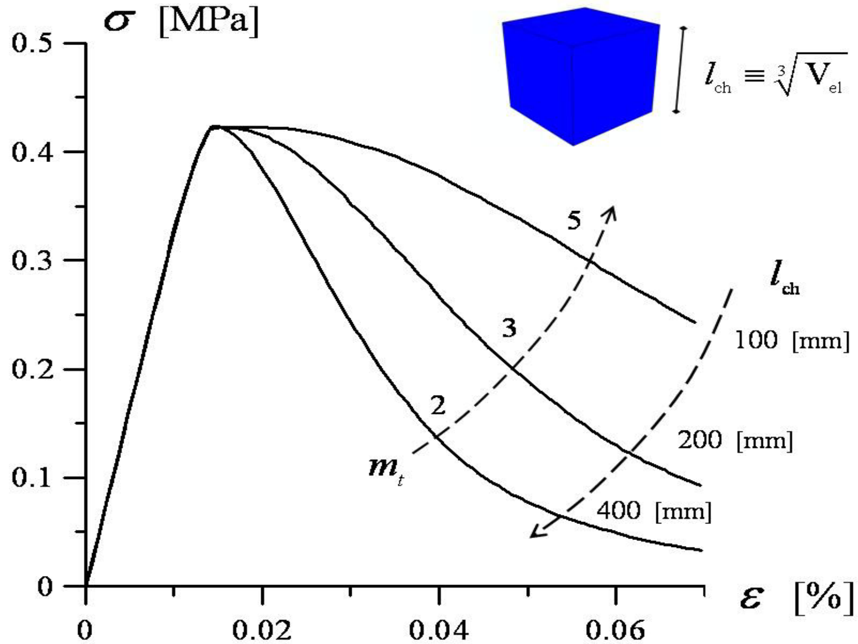

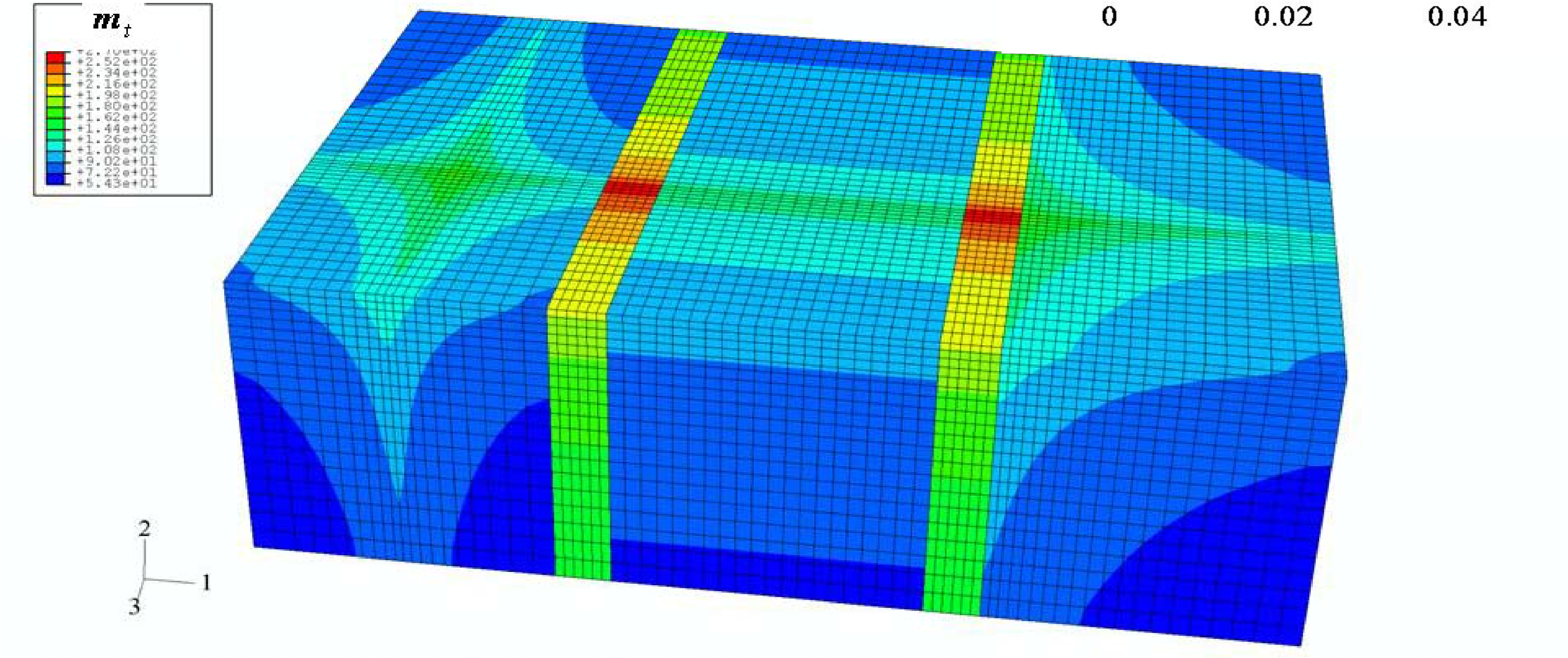

Table

Model parameter	Meaning	**Brick**	**Mortar**
E	Young modulus	4250 MPa	5000 MPa
ν	Poisson ratio	0.1	0.1
a_t	parameter governing tensile damage activation function f_t	0.329	0.12
b_t	parameter governing tensile damage activation function f_t	3.78 MPa	2.4 MPa
k_t	parameter governing tensile damage activation function f_t	6.2 MPa^2	10.5 MPa^2
$(\sigma_{et}/\sigma_{0t})$	uniaxial stress at the elastic limit / uniaxial peak stress, in tension	0.8	0.8
D_{0t}	tensile damage at peak	0.1	0.1
a_c	parameter governing compressive damage activation function f_c	0.0025	0.0025
b_c	parameter governing compressive damage activation function f_c	2.75 MPa	1.1 MPa
k_c	parameter governing compressive damage activation function f_c	36 MPa^2	28 MPa^2
$(\sigma_{ec}/\sigma_{0c})$	uniaxial stress at the elastic limit / uniaxial peak stress, in compression.	0.7	0.7
D_{0c}	compressive damage at peak	0.3	0.3
G_t	fracture energy in tension	0.14 N/mm	0.09 N/mm
G_c	fracture energy in compression	14 N/mm	9 N/mm

Table 1: Damage model parameters adopted for the historical bricks and high-strength mortar joints.

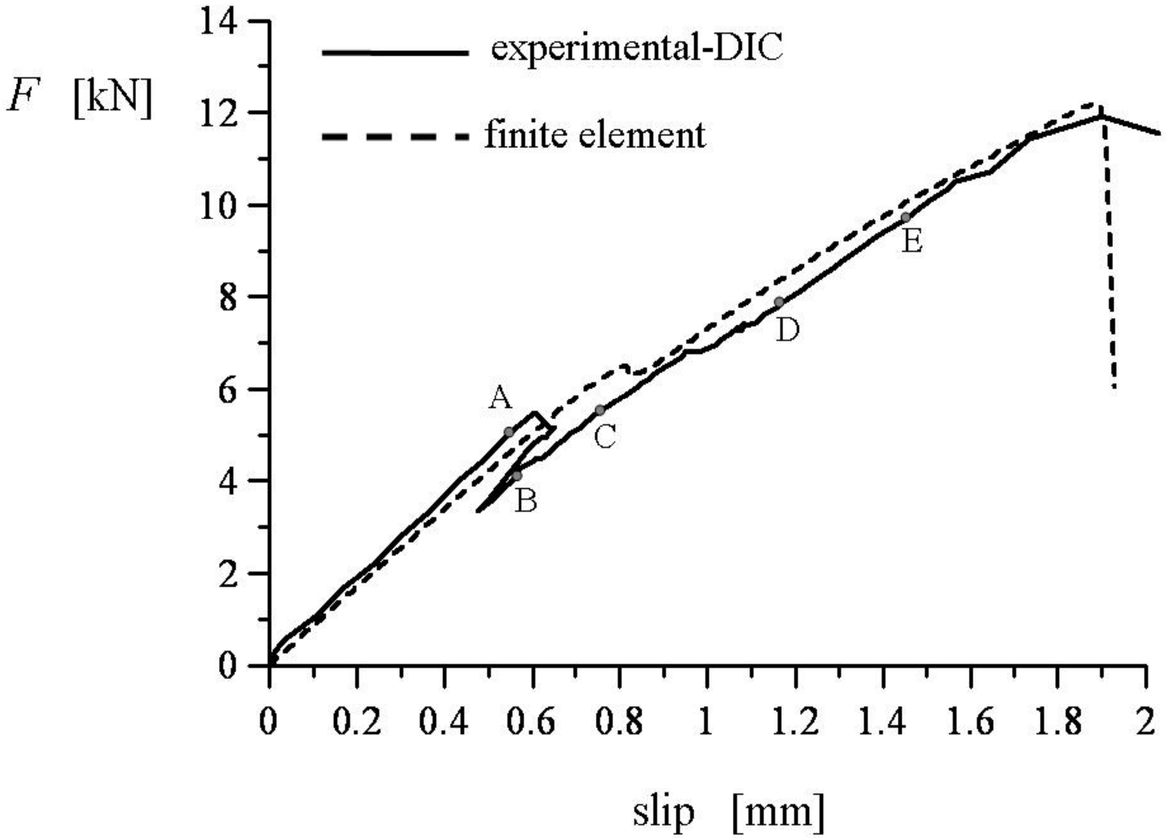

F [kN]
14
12
10
8
6
4
2
0
experimental-DIC
finite element
A
B
C
D
E
0
0.2
0.4
0.6
0.8
1
1.2
1.4
1.6
1.8
2
slip [mm]

Local predictions of FE model

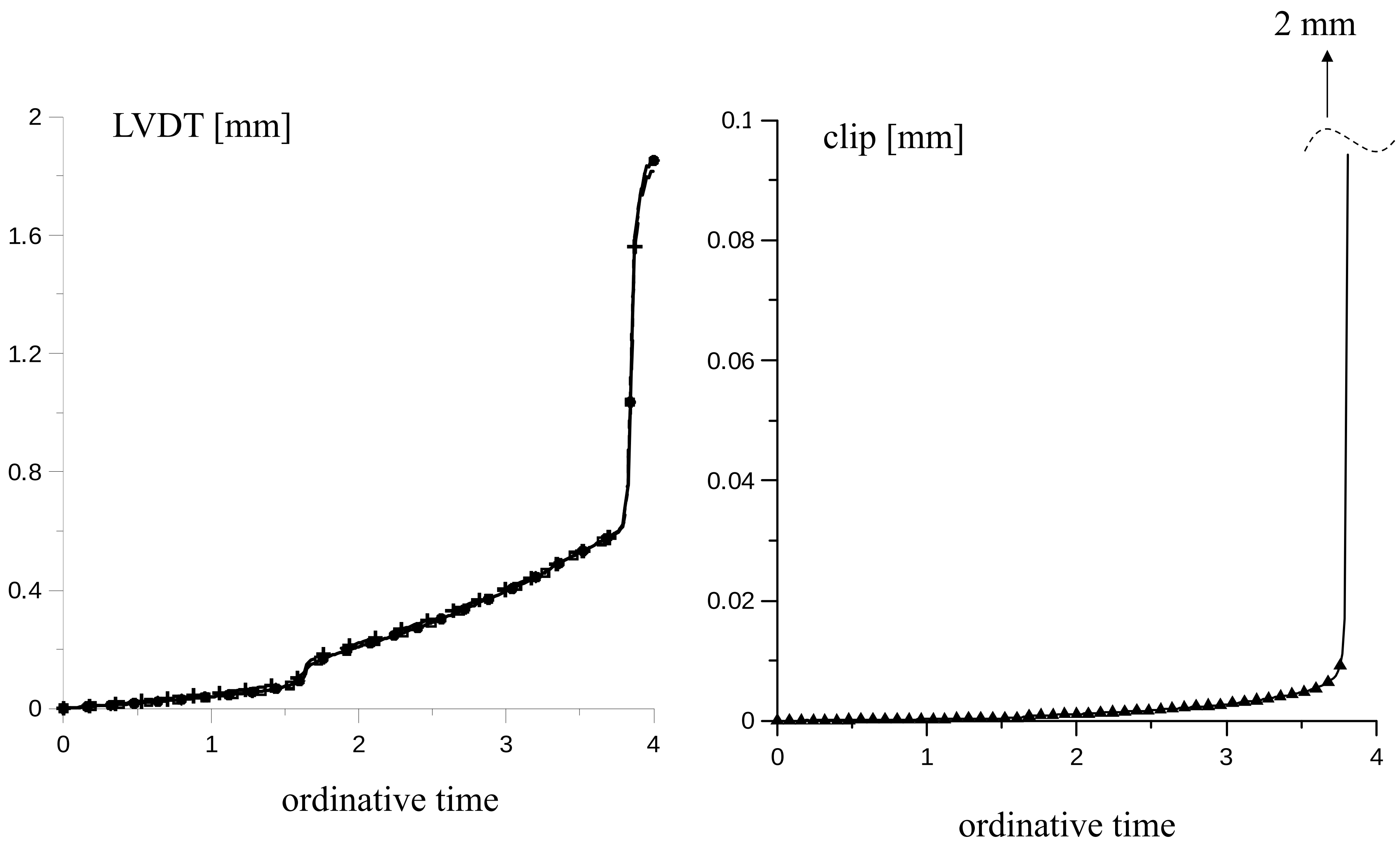

Closing remarks

- Single-lap shear tests were performed under clip-control
- Delamination of CFRP strips from a small masonry pillar was simulated under the hypothesis of a perfect adhesion.
- 3D heterogeneous FE model with elastic-damageable phases was developed
- Optical monitoring was validated with correction of optical distorsion
- Information fusion
- Future prospects: combining interface and bulk damage

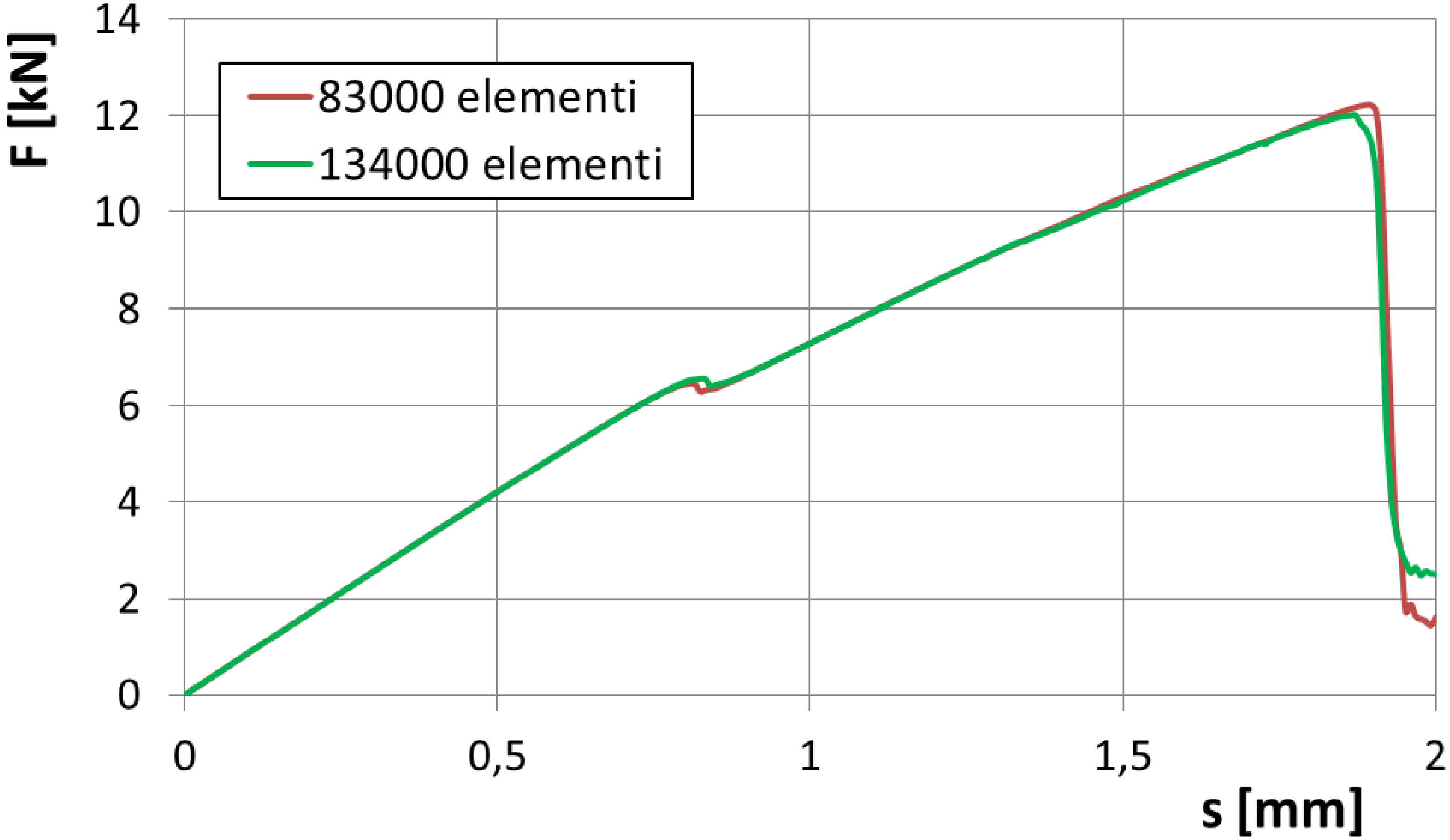

F [kN]
14
12
10
8
6
4
2
0
83000 elementi
134000 elementi
0
0,5
1
1,5
2
s [mm]

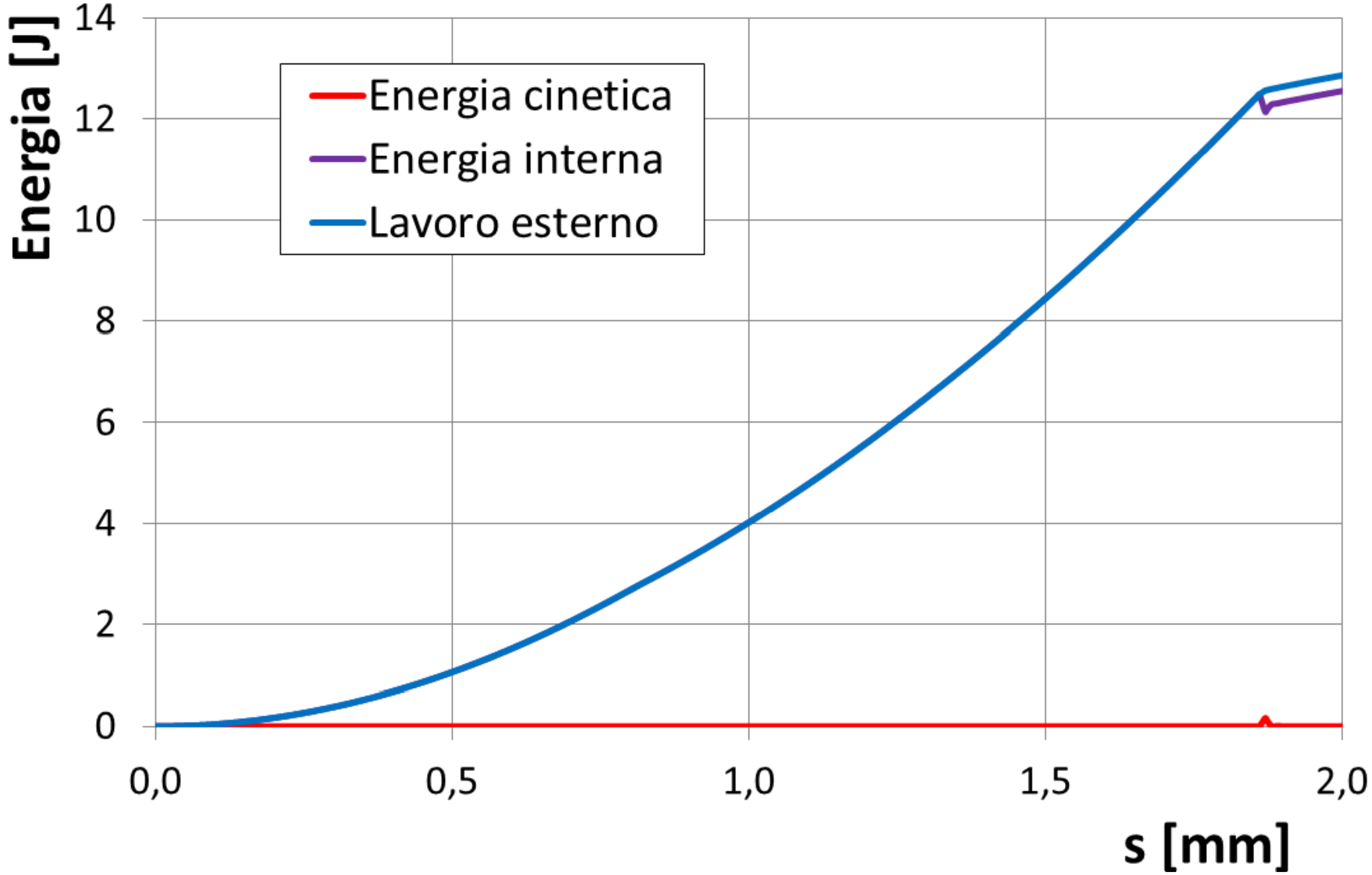

Energia [J]
14
12
10
8
6
4
2
0
Energia cinetica
Energia interna
Lavoro esterno
0,0
0,5
1,0
1,5
2,0
s [mm]

Local traction predicted by FEM

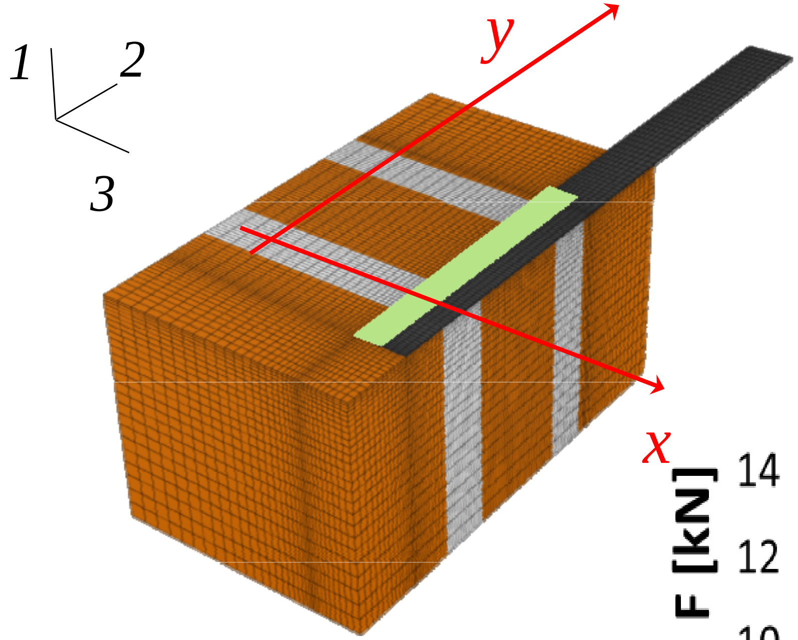

$$\overline{\tau} = \frac{F_{max}}{A} \approx 1.7 \ \text{MPa}$$

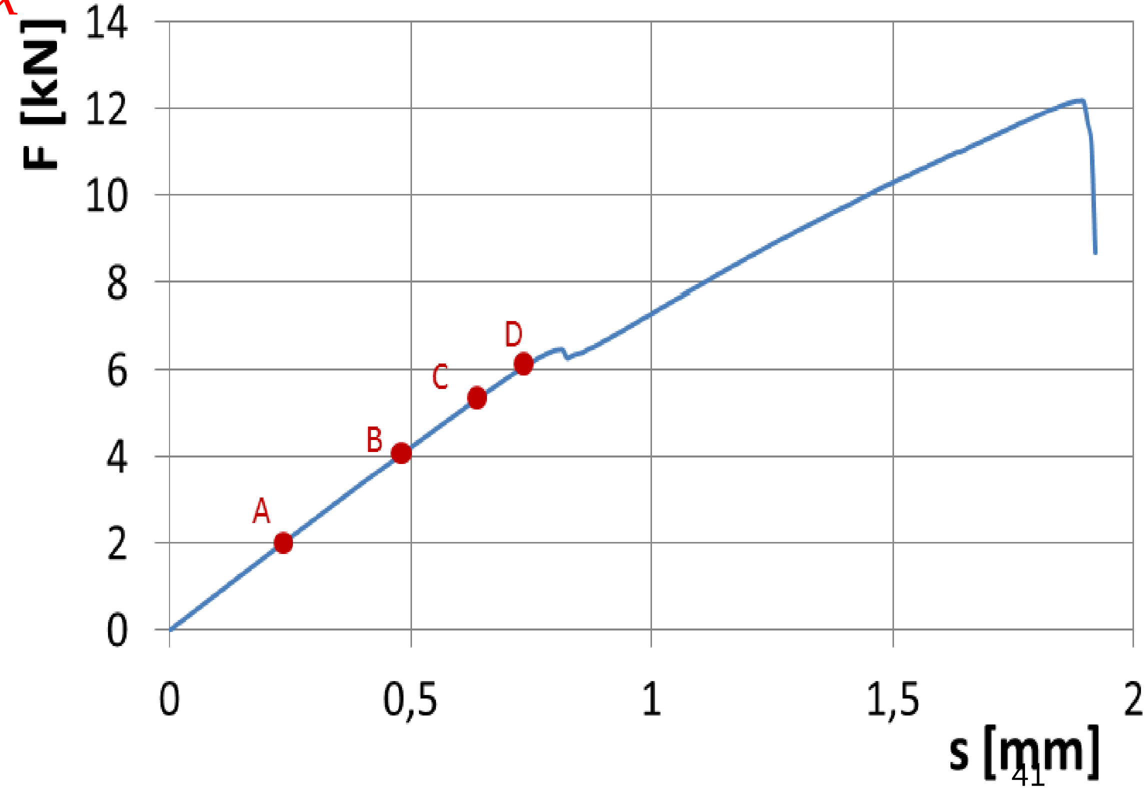

FEM

τ_{12}

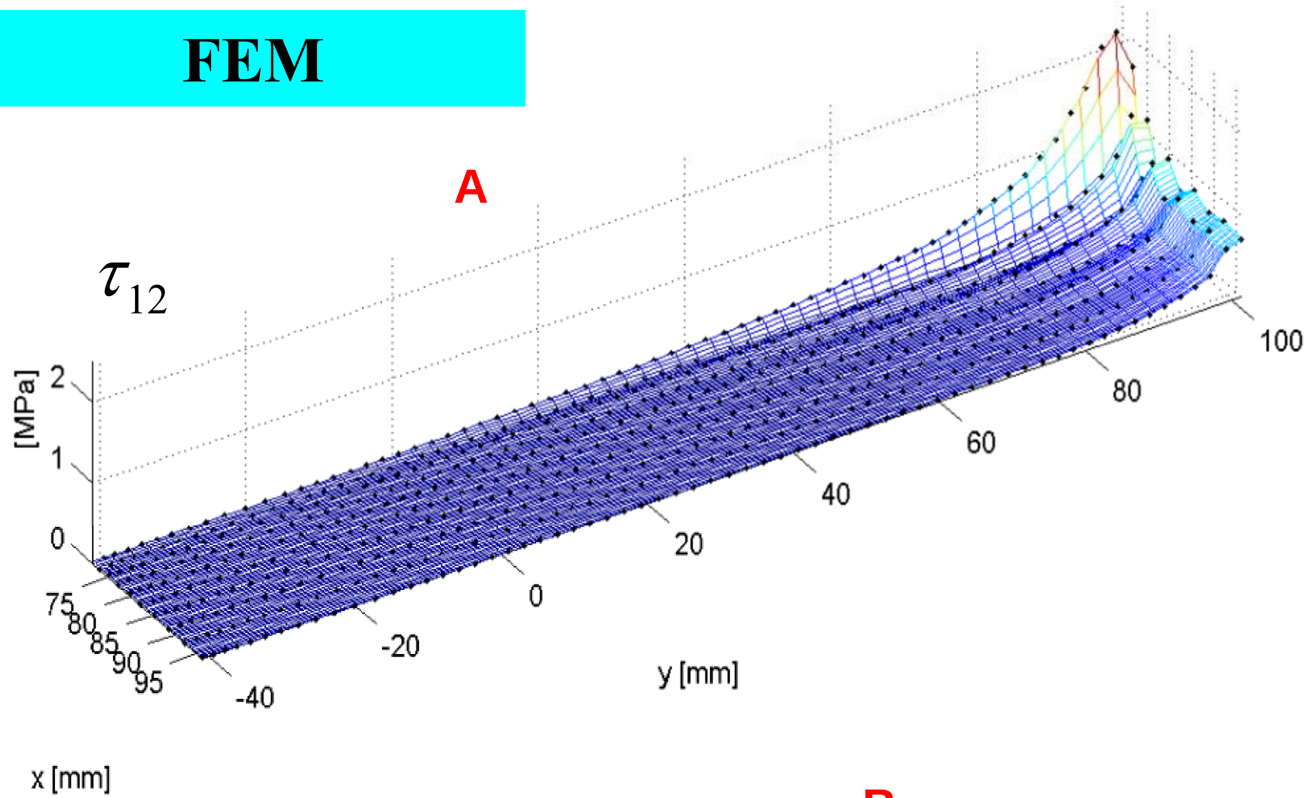

delamination front

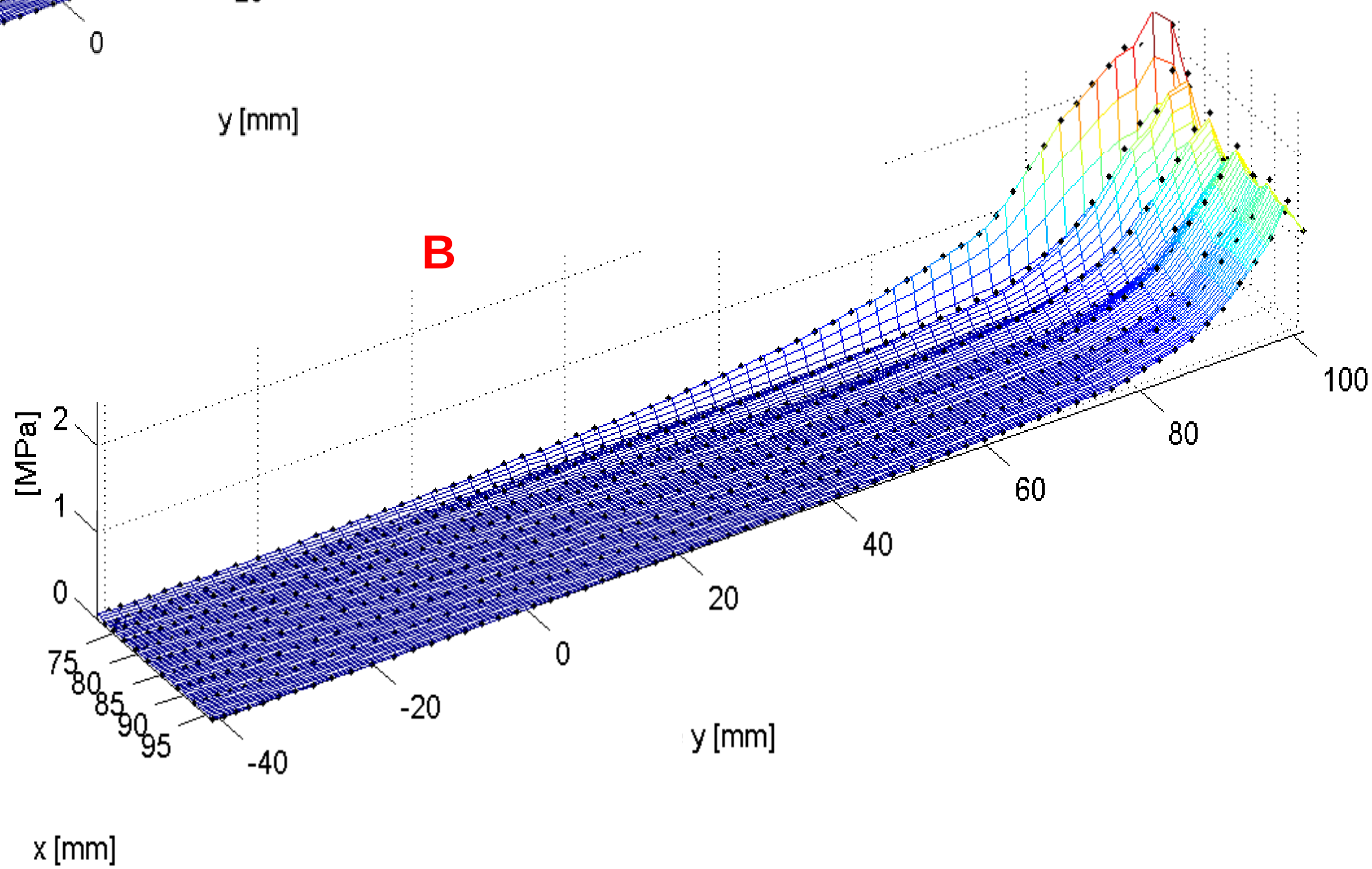

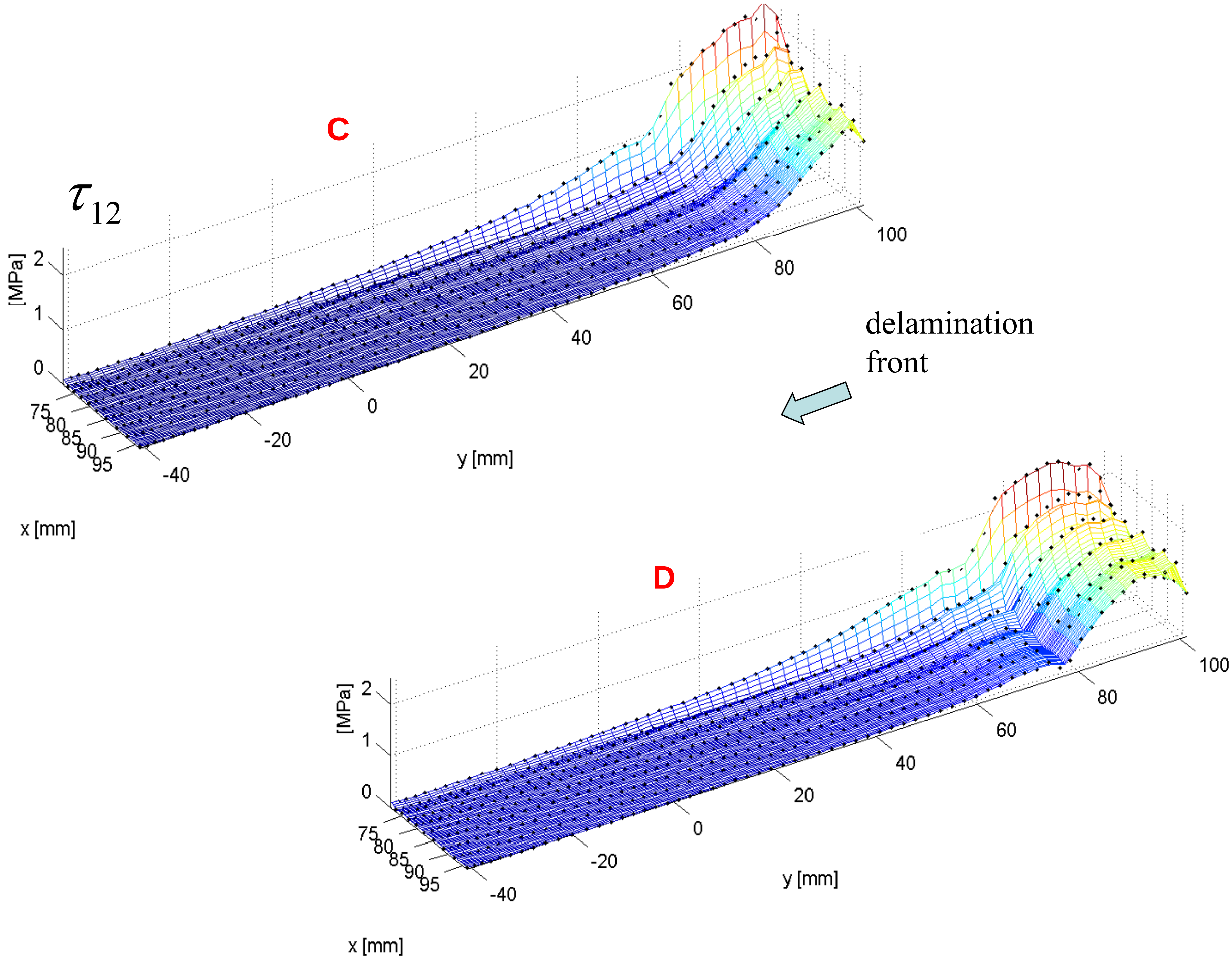

τ_{12}
C
D
[MPa]
2
1
0
75
80
85
90
95
-40
-20
0
20
40
60
80
100
y [mm]
x [mm]
delamination front

A priori assumed parameters ("diffuse load cell")

Ceramic phase CFC SEP NB31: Mechanical parameters at room temperature		
Elastic properties	Hill parameters for plastic anisotropy	Ramberg-Osgood parameters for the incompressible strains
$E_x = 107\,[\text{GPa}]$; $E_y = 15\,[\text{GPa}]$; $E_z = 12\,[\text{GPa}]$; $\nu_{xy} = 0.10$; $\nu_{xz} = 0.20$; $\nu_{yz} = 0.20$; $G_{xy} = 10\,[\text{GPa}]$	$\mathcal{F} = 0.8$; $\mathcal{G} = 0.5$; $\mathcal{H} = 0.5$; $\mathcal{N} = 10$;	$\sigma_0 = 100\ [\text{MPa}]$; $E_R / \alpha = 2083\ [\text{GPa}]$; $n = 7$;

Cu phase: Mechanical parameters at room temperature	
Elastic properties	Ramberg-Osgood parameters
$E = 125\,[\text{GPa}]$; $\nu = 0.34$;	$\sigma_0 = 300\ [\text{MPa}]$; $\alpha = 0.06$; $n = 7$;

Ref: ITER Final Report, Material Assessment Report, 2001

Post-mortem analyses of fracture surface by SEM

Failure of CFC by interlaminar shear,
carbon fibre pull-out and cracking of CCr

c)

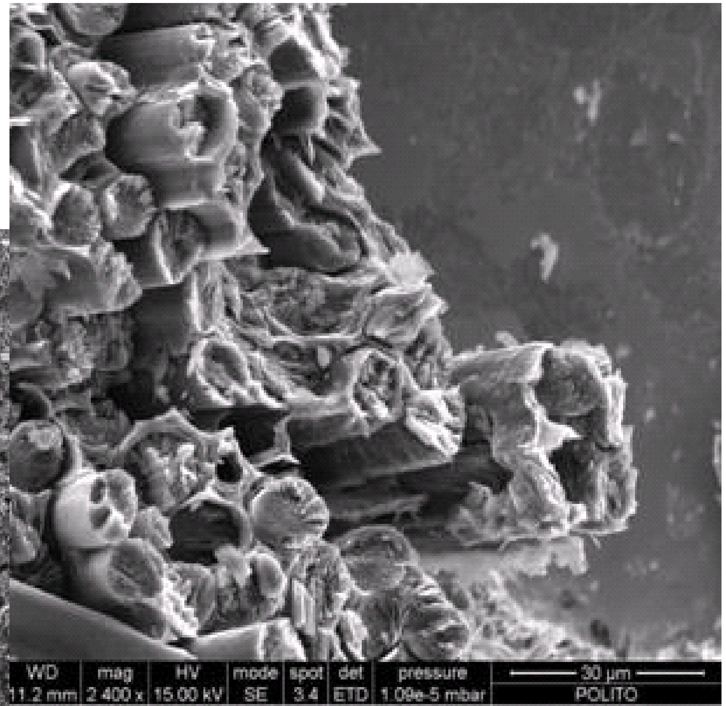

b)

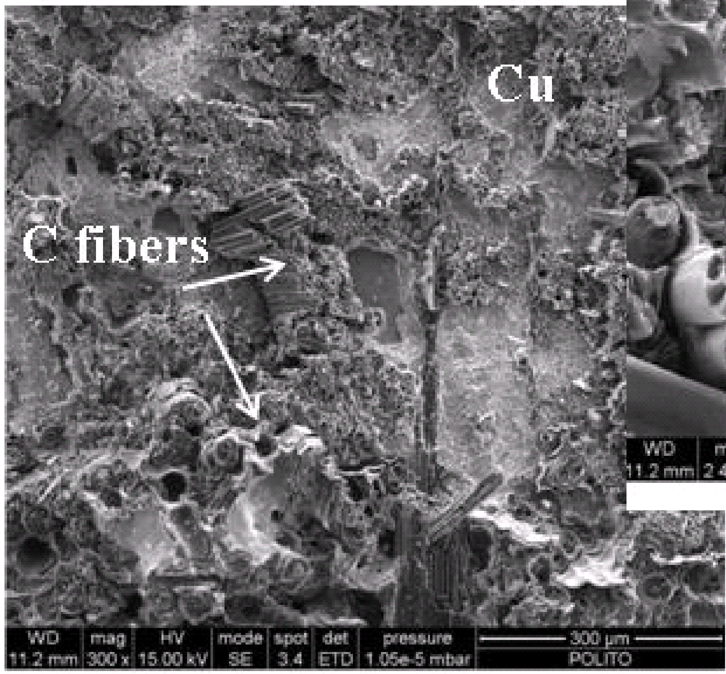

a)

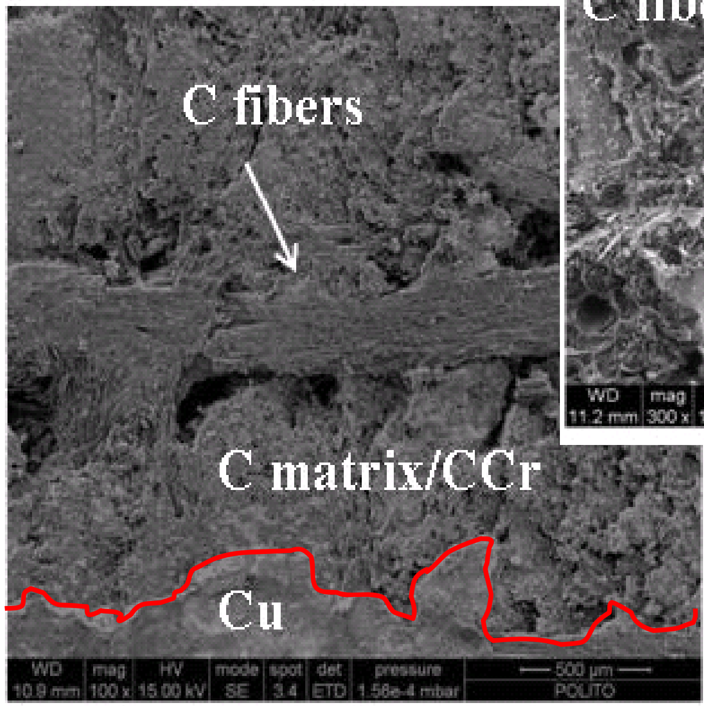

SEM
pictures

resolution

ITER Final Design Report (July 2001): Materials

Table 2.3-3 Properties of SEP NB31 [11]

Properties	T, °C	x	y	z
Thermal conductivity, W/mK	RT 800 1000 1500	323 154 145 136	117 58 56 55	115 55 52 51
Specific Heat, J/kg K	RT 800 1000		780 1820 2000	
CTE, 10^{-6} K^{-1}	800 1000	0.4 0.5	1 1.2	2.1 2.7
Tensile strength, MPa	RT	130	30	19
Tensile strain, %	RT	0.14	0.30	/
Young Modulus, GPa	RT	107	15	/
Poisson's ration	RT	xz: 0.2 xy: 0.1		yz: 0.2 yx: 0.1
Compressive strength, MPa	RT	102	31	/
Shear strength, MPa	RT	xz: 15		yz: 9
Electrical resistivity, μΩm	RT	3.7	12.4	
Density, kg/m^3	RT		1900	
Porosity, %	RT		8	

Flat-tile mock-ups manufacturing

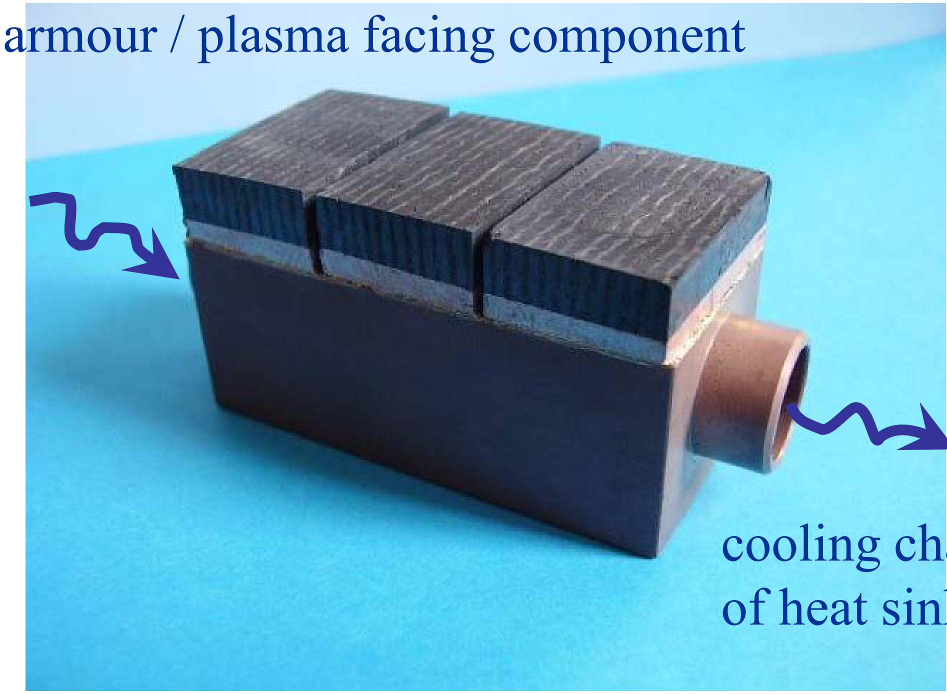

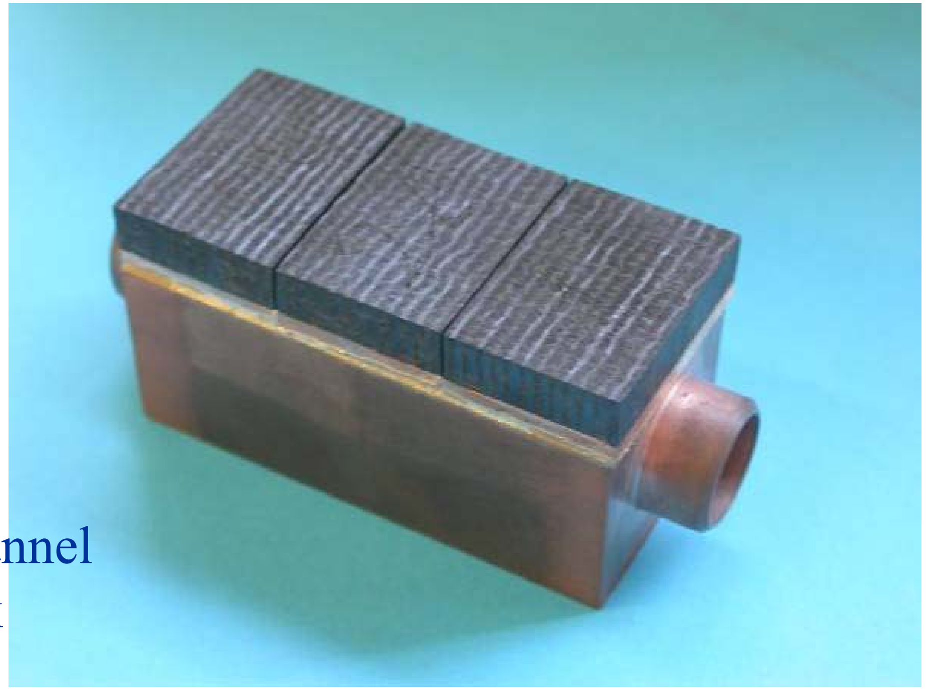

CFC NB31/Cu/CuCrZr

1) High heat flux applied on CFC surface
up to 10 MW/m^2 (3000 cycles)
up to 20 MW/m^2 during transient events (20 cycles)

2) Neutron irradiation and radiation damage

Problems when joining metals and CFC

- Large thermal expansion mismatch

  between Cu and CFC

  α_{CFC}=1,7-3,3 x 10^{-6} K^{-1},

  α_{Cu}=16,6 x 10^{-6} K^{-1}

  → high residual stresses

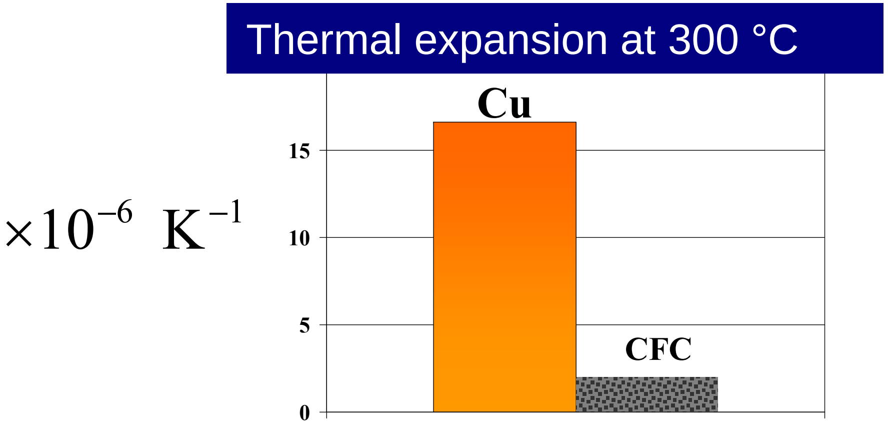

- Low wettability of molten copper

on CFC (contact angle= 140°)

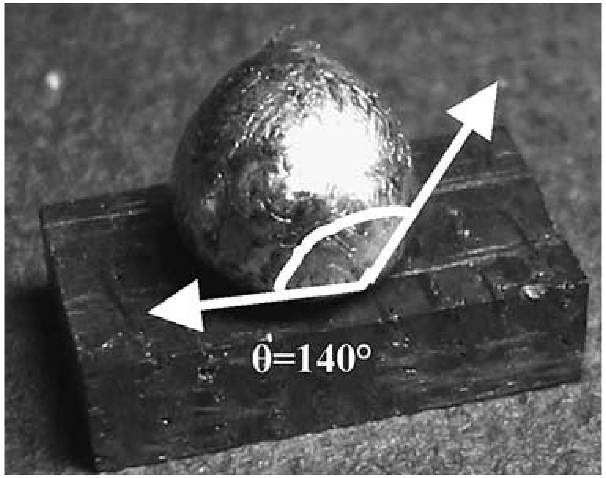

sessile drop test
at 1100 °C
for 30 min
under Argon

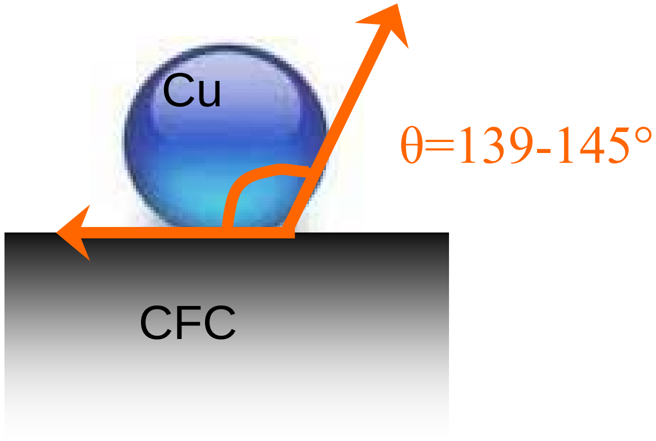

Joint manufacturing by one-step brazing

Ferraris et alii, J. Nucl Mat. 2008

1. Composite surface is modified by direct reaction with chromium → a carbide layer is formed: large reduction of the C/C-Cu contact angle.

2. Commercial brazing alloy (Gemco®) is used to braze C/C to pure copper and pure copper to CuCrZr by the same heat treatment. Alloy does not contain any activating element (such as Ti and Si)

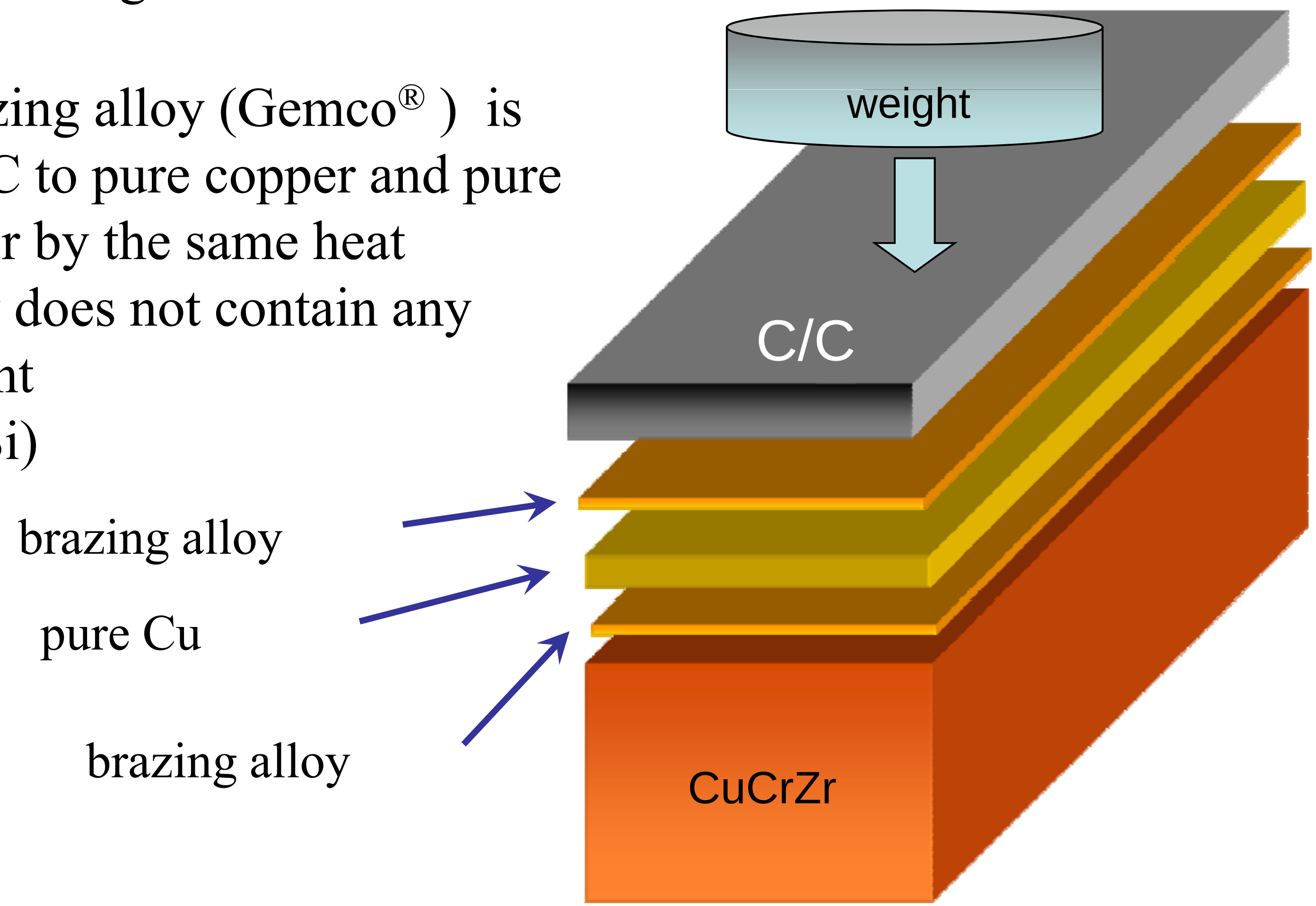

2D- Digital Image Correlation

"passive" advection of the local texture
(optical flow conservation)

displacement vector

local form

$$f(\mathbf{x}) \simeq g(\mathbf{x} + \mathbf{u}[\mathbf{x}])$$

reference image

deformed image

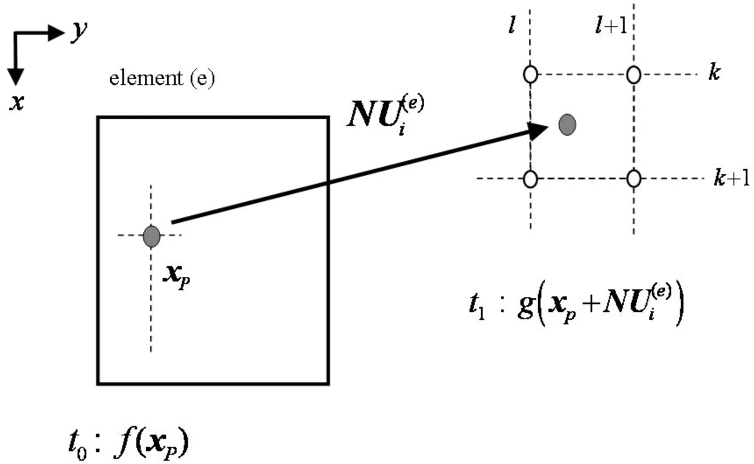

weak form

similarity measure

$$\arg\min_{\mathbf{u}} \left\{ \eta(\mathbf{u}) = \int_{\Omega} \left[f(\mathbf{x}) - g(\mathbf{x} + \mathbf{u}) \right]^2 d\mathbf{x} \right\}$$

variational problem

$$\mathbf{u}_{i+1} = \mathbf{u}_i + \delta\mathbf{u}_{i+1}$$ incremental form

Truncated expansion and stationarity

Euler-Lagrane stationarity condition $\delta\eta_2 = \langle \operatorname{grad}\eta_2, \delta\mathbf{v}_{i+1} \rangle = 0 \quad \forall\, \delta\mathbf{v}_i \in \mathbf{L}_2$

$$a(\delta\mathbf{u}_{i+1}, \delta\mathbf{v}_{i+1}) = 2\int_\Omega \delta\mathbf{v}_{i+1}^T \boxed{\nabla g \cdot \nabla g^T}\, \delta\mathbf{u}_{i+1}\, d\mathbf{x}$$

$$\mathcal{K} = \nabla g \cdot \nabla g^T$$

bilinear form

$$F(\delta\mathbf{v}_{i+1}) = 2\int_\Omega \delta\mathbf{v}_{i+1}^T \nabla g \left[g(\mathbf{x} + \mathbf{u}_i) - f(\mathbf{x}) \right] d\mathbf{x}$$

linear form

$$\mathbf{L}_2(\Omega) \equiv L_2 \times L_2 \times L_2$$

$$\text{find } \delta\mathbf{u}_i \in \mathbf{L}_2 : \quad a(\delta\mathbf{u}_i, \delta\mathbf{v}_i) = F(\delta\mathbf{v}_i) \quad \forall\, \delta\mathbf{v}_i \in \mathbf{L}_2$$

semi-coercive variational problem

multiplicity of solution $\mathbf{u}_0 + \operatorname{Ker}\mathcal{K}$

Galerkin finite-element discretization

$u = NU^{(e)}$

$$\boxed{\mathbf{K} \cdot \delta\mathbf{U}_{i+1} = \mathbf{B}}$$

pseudo-stiffness

pseudo-load

Tangential traction and 95% confidence strip

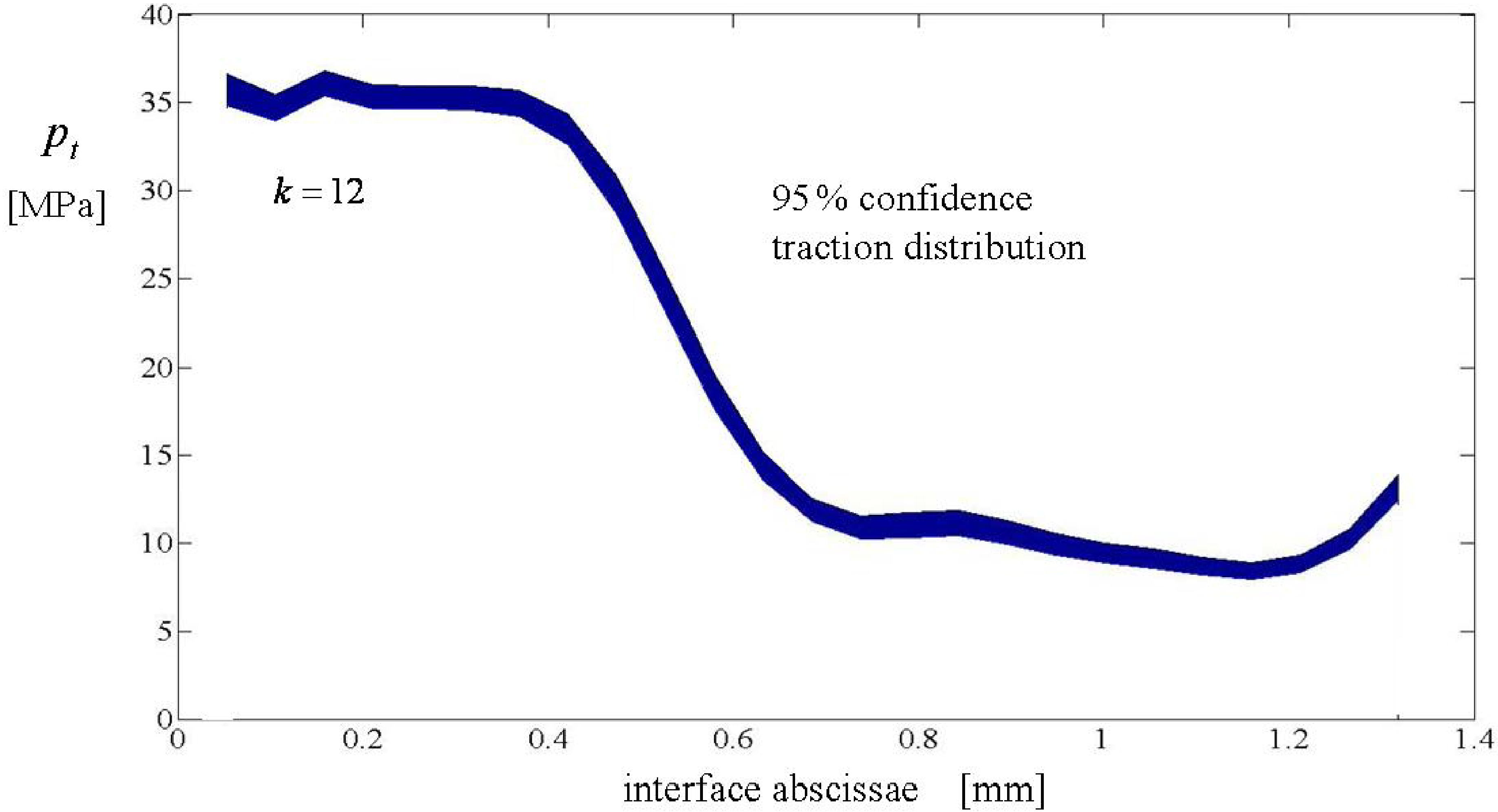

Normal traction and 95% confidence strip

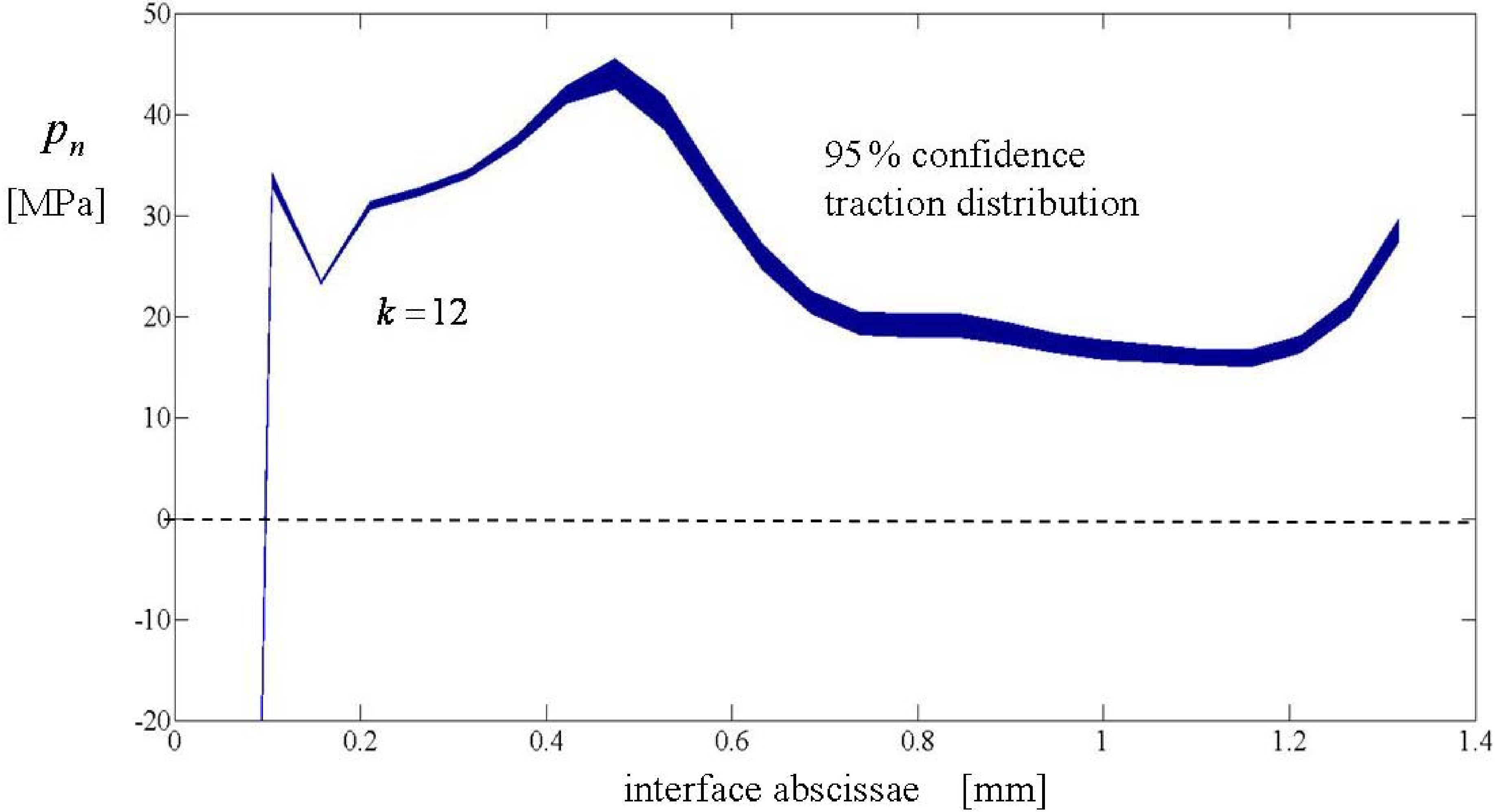

Parameter sensitivity of displacement field

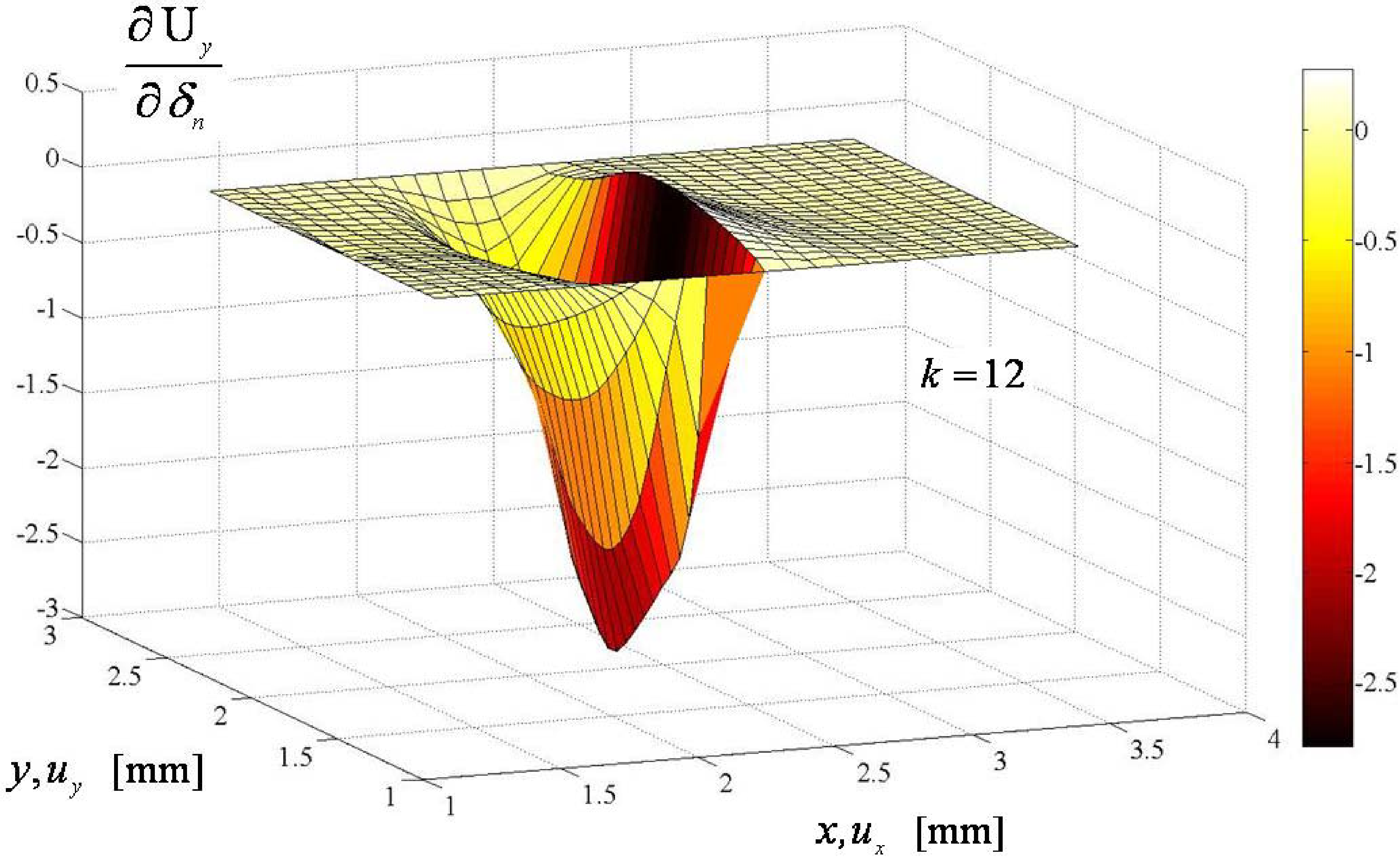

Estimate dependence on a priori information

variance assessment by σ-point strategy

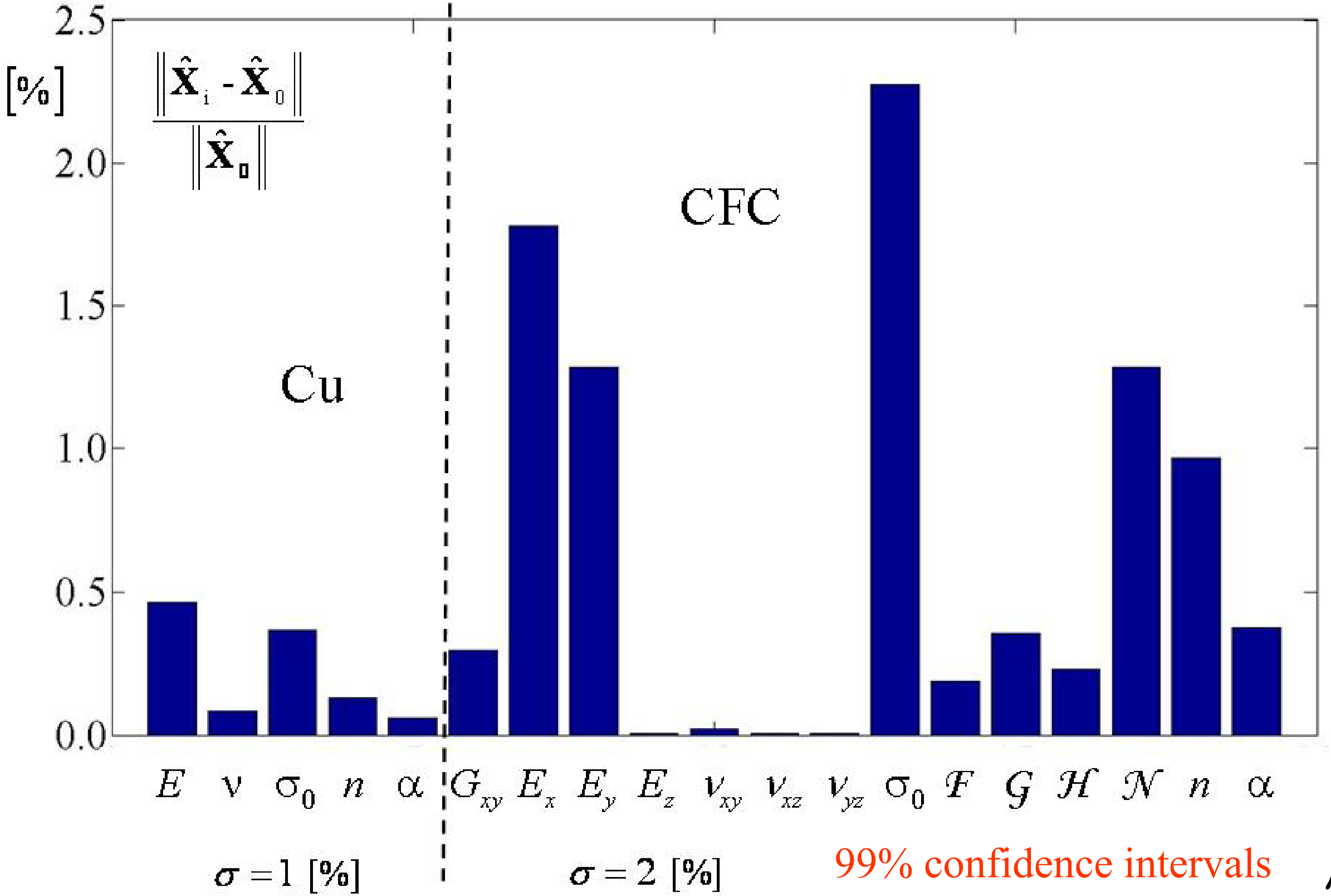

99% confidence intervals $\mu \pm 3\sigma$

Confidence ellipsoids and Bonferroni's domains

$\overline{\phi_n} = 0.106$ [GPa $\cdot\,\mu$m]

$\overline{\delta_t} = 10.7$ [μm] $\overline{\delta_n} = 0.665$ [μm]

$$(\mathbf{X} - \overline{\mathbf{X}})^T\ \overline{\mathbf{C}}_{\mathrm{X}}^{-1}\ (\mathbf{X} - \overline{\mathbf{X}}) = \chi^2_{n_{\mathrm{X}},1-\alpha}$$

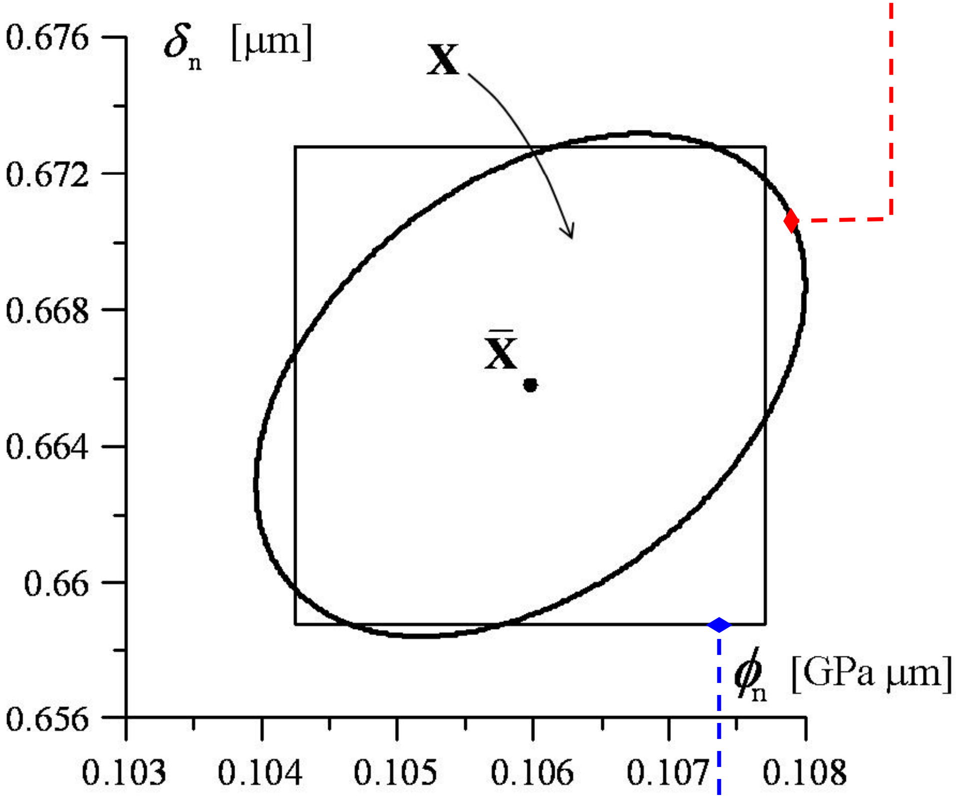

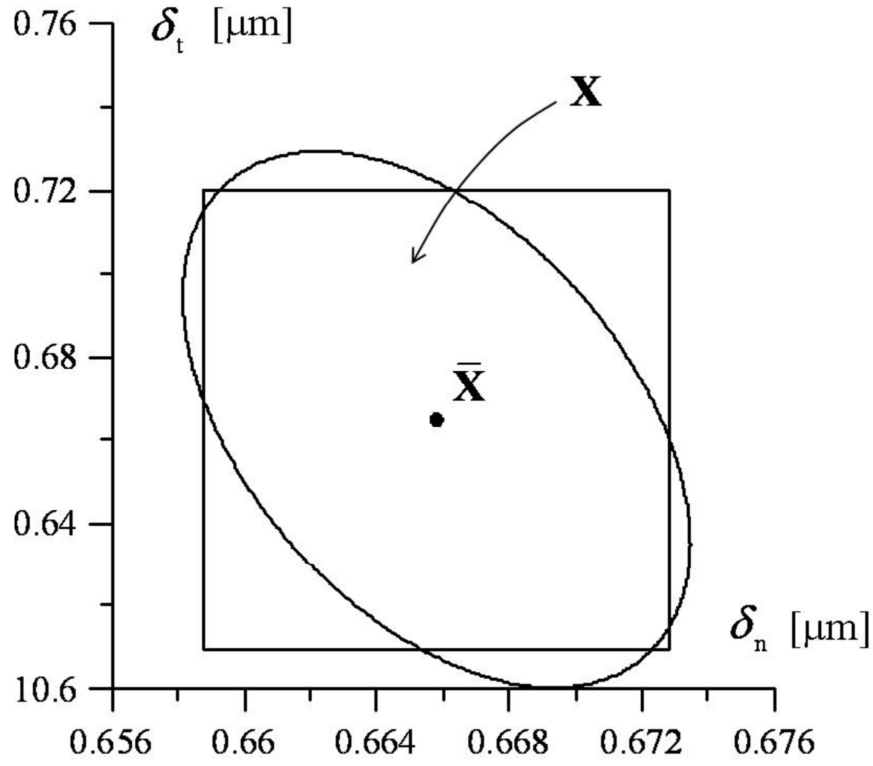

equivalent parallelipedic domains

$$\overline{X}_i + z_{\alpha^*} \cdot \sqrt{\overline{C}_{\mathrm{X}_{ii}}} \le X_i \le \overline{X}_i + z_{1-\alpha^*} \cdot \sqrt{\overline{C}_{\mathrm{X}_{ii}}}$$

$(i = 1,2,3)$ $\alpha^* = \alpha / (2n_{\mathrm{X}})$

Engineering motivations

- The behavior of masonry structures, strengthened with fiber-reinforced polymer (FRP) thin sheets, is often dominated by delamination of the FRP reinforcement from the support.

- A further complication is the presence of mortar joints, where cracks may propagate preferentially.

- This fundamental issue is relatively under-investigated for masonry, especially from a numerical point of view.

Items to be discussed

- engineering motivations
- shear tests on joined CFC/Cu assemblies
- “optical” inverse problem:
  from pictures to displacements
  through 2D Digital Image Correlation
- “mechanical” inverse problem:
  from full field data to joint properties
  through Finite Element Model Updating
- closing remarks and future prospects

Ceramic Matrix Composite SEP NB31

NOVOLTEX® preform

PAN=Poly-Acrylo-Nitrile

1

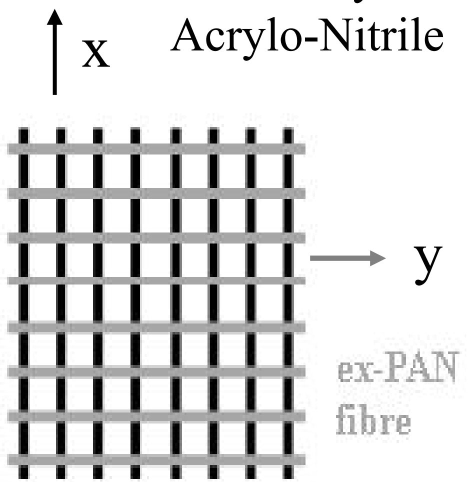

ex-pitch fibre

2

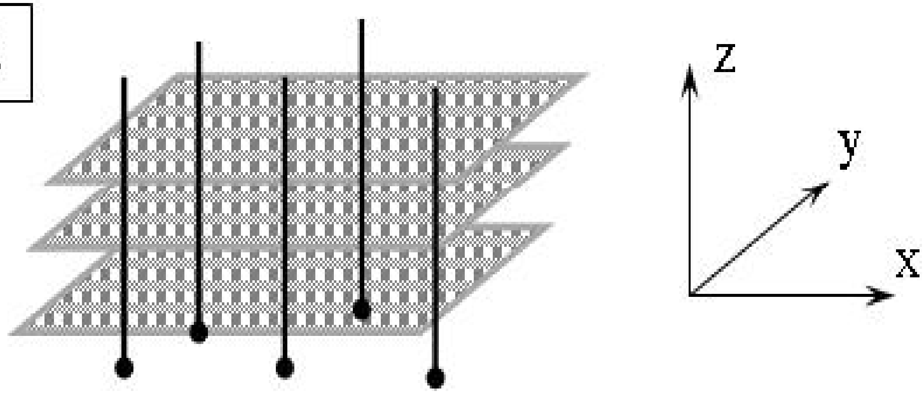

needling (PAN-fibers)

3

isothermal chemical vapour infiltration → graphitisation → liquid impregnation

several times

4

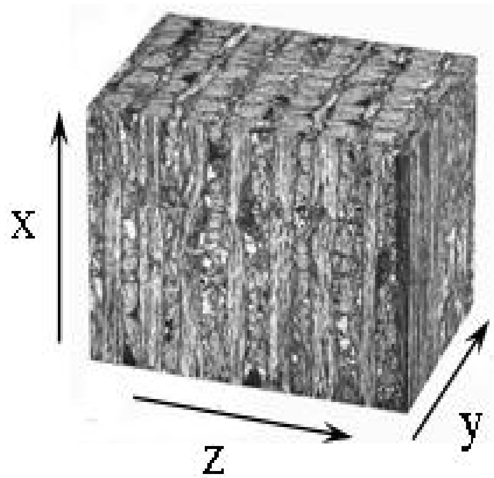

SEM (Philips 525 M)

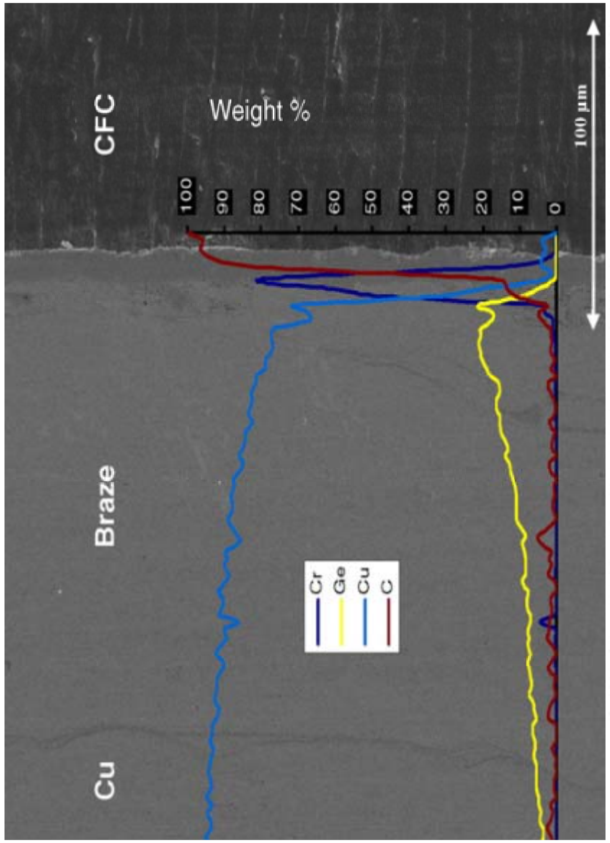

Energy Dispersive
X-ray spectroscopy

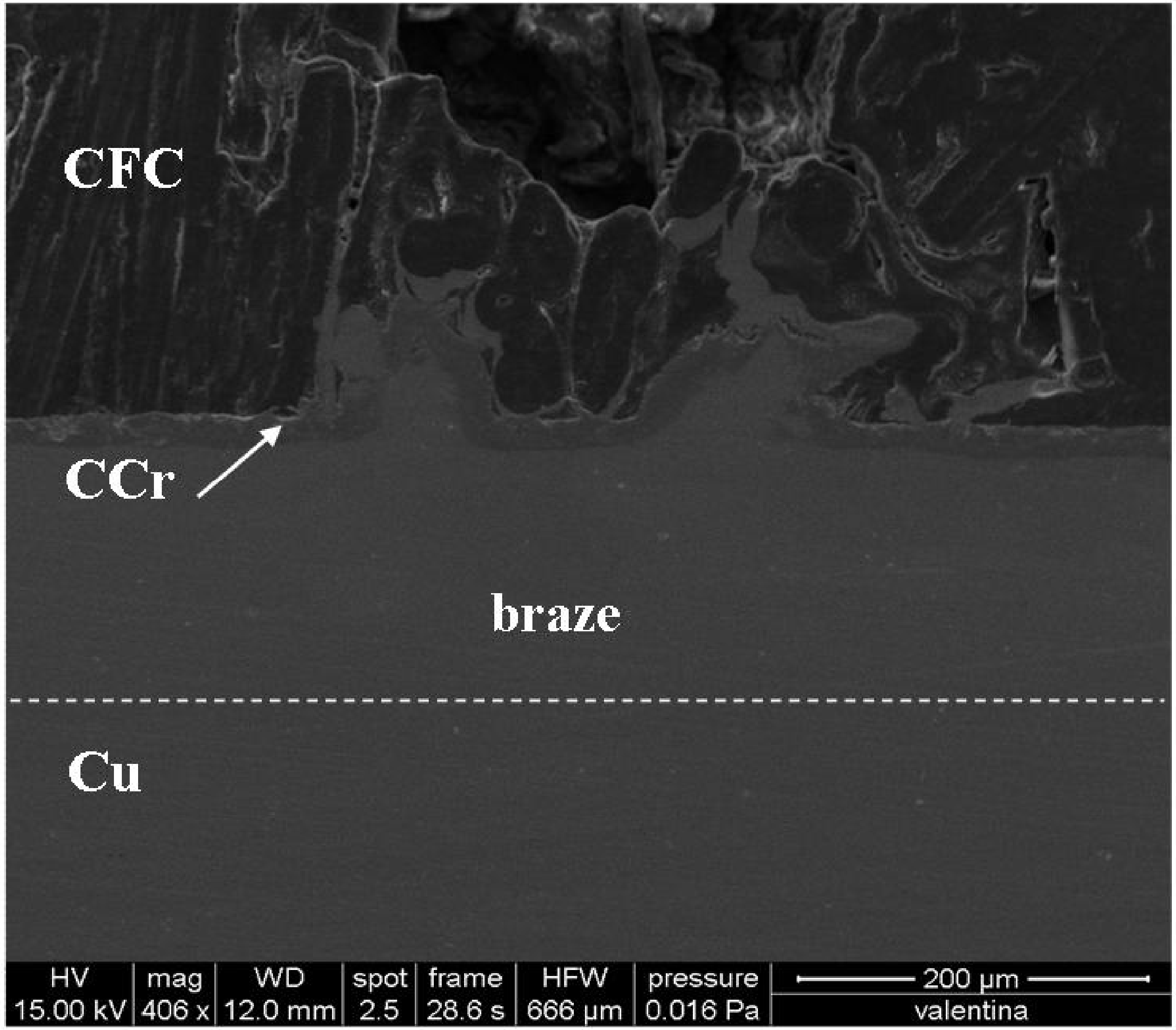

Cromium carbide (about 20 µm thick)
Cr_7C_3 and $Cr_{23}C_6$

Adherent nonlinear behavior under plane stress

anisotropic extension of multiaxial Ramberg-Osgood relationship

Műcke & Bernhardi
CMAME (2003)

3 parameters

$$\boldsymbol{\varepsilon} = \boldsymbol{\varepsilon}_{\text{el}} + \boldsymbol{\varepsilon}_{\text{pl}} = \mathcal{C}\,\boldsymbol{\sigma} + \frac{\alpha}{E_R}\left[\frac{\sigma_{\text{eq}}^{n-1}}{\sigma_0^{n-1}}\right]\mathcal{M}\,\mathbf{s}$$

deviatoris stress tensor

$$\mathbf{s} \equiv \boldsymbol{\sigma} - (\operatorname{tr}\boldsymbol{\sigma}/3)\,\mathbf{1}$$

$$\sigma_{\text{eq}} \equiv \left(\mathbf{s}^T\,\mathcal{M}\,\mathbf{s}\right)^{1/2}$$ equivalent stress

$$\sum \mathcal{M}([1:3],[1:3]) = 0$$

$$\mathcal{C} \equiv \begin{pmatrix} 1/E_x & -\nu_{yx}/E_y & -\nu_{zx}/E_z & 0 \\ -\nu_{xy}/E_x & 1/E_y & -\nu_{zy}/E_z & 0 \\ -\nu_{xz}/E_x & -\nu_{yz}/E_y & 1/E_z & 0 \\ 0 & 0 & 0 & 1/G_{xy} \end{pmatrix}$$

$$\mathcal{M} \equiv \begin{pmatrix} \mathcal{G}+\mathcal{H} & -\mathcal{H} & -\mathcal{G} & 0 \\ -\mathcal{H} & \mathcal{H}+\mathcal{F} & -\mathcal{F} & 0 \\ -\mathcal{G} & -\mathcal{F} & \mathcal{F}+\mathcal{G} & 0 \\ 0 & 0 & 0 & 2\mathcal{N} \end{pmatrix}$$

3 parameters

$$\nu_{ij}/E_i = \nu_{ji}/E_j \qquad i, j = x, y, z$$

incompressible strain $\operatorname{tr}(\boldsymbol{\varepsilon}_{\text{pl}}) = 0$

7 parameters

for isotropic Cu $\mathcal{F} = \mathcal{G} = \mathcal{H} = \frac{1}{2};\ \mathcal{N} = \frac{3}{2}$

First-order sensitivity analysis by Direct Differentiation Method

unknown parameters

FE equilibrium eqs
at the free dofs
at step *n*

$$\mathbf{F}_{\text{int}}\left(\mathbf{X};\mathbf{U}^{n}(\mathbf{X});\bar{\mathbf{U}}^{n}_{\partial\Omega}\right)=\mathbf{0}$$

Here dependence
only upon $\mathbf{U}^{n}$

prescribed displacements
along the boundary

$$\frac{\partial}{\partial\mathbf{X}^{T}}\mathbf{F}_{\text{int}}=\left(\frac{\partial\mathbf{F}_{\text{int}}}{\partial\mathbf{U}^{n}}\right)\frac{\partial\mathbf{U}^{n}}{\partial\mathbf{X}^{T}}+\frac{\partial\mathbf{F}_{\text{int}}}{\partial\mathbf{X}^{T}}=\mathbf{0}$$

pseudo-load vector

$$\boxed{\mathbf{K}_{\tan}\frac{\partial\mathbf{U}^{n}}{\partial\mathbf{X}^{T}}=\left(-\frac{\partial\mathbf{F}_{\text{int}}}{\partial\mathbf{X}^{T}}\right)}$$

assembled tangent stiffness matrix,
already available in a Newton scheme